Compact Integrated Designs of Microwave Filters and Antennas with Dual-Polarization

by

Zainab Maqsood

A thesis submitted to the

School of Graduate and Postdoctoral Studies in partial

fulfillment of the requirements for the degree of

Master of Applied Science in Electrical and Computer Engineering

The Faculty of Engineering and Applied Science

University of Ontario Institute of Technology (Ontario Tech University)

Oshawa, Ontario, Canada

February, 2021

THESIS EXAMINATION INFORMATION

Submitted by: **Zainab Maqsood**

Master of Applied Science in **Electrical and Computer Engineering**

Thesis title: Compact Integrated Designs of Microwave Filters and Antennas with Dual Polarization

An oral defense of this thesis took place on February 4th, 2021 in front of the following examining committee:

Examining Committee:

Chair of Examining Committee	Dr. Jing Ren
Research Supervisor	Dr. Ying Wang
Research Co-supervisor	Dr. Langis Roy
Examining Committee Member	Dr. Ming Yu
Thesis Examiner	Dr. Min Dong

The above committee determined that the thesis is acceptable in form and content and that a satisfactory knowledge of the field covered by the thesis was demonstrated by the candidate during an oral examination. A signed copy of the Certificate of Approval is available from the School of Graduate and Postdoctoral Studies.

ABSTRACT

Microwave antenna and filter circuits are key components in all types of communication systems. In order to achieve high compactness and high performance for next generation wireless networks, this thesis investigates the use of a material with a high dielectric constant (approximately 20) and low loss for integrated design of microwave filters and antennas. Two different filtering antenna designs in the 3.5 – 3.7 GHz frequency range are presented. A dual-mode waveguide filter is used in both designs, while a microstrip antenna is used for one design and a dielectric resonator antenna (DRA) is used for the other. Microstrip antenna and DRA are used due to their low-profile, ease of fabrication and light weight. The integrated designs are validated using full wave electromagnetic (EM) simulations, showing comparable performances. Both designs are compact, low loss, and have dual-polarization with good isolation, making them ideal for 5G mobile communication applications.

Keywords: Filter antenna integration; dual-polarization; dielectric resonator antennas; microstrip antennas.

AUTHOR'S DECLARATION

I hereby declare that this thesis consists of original work of which I have authored. This is a true copy of the thesis, including any required final revisions, as accepted by my examiners.

I authorize the University of Ontario Institute of Technology to lend this thesis to other institutions or individuals for the purpose of scholarly research. I further authorize University of Ontario Institute of Technology to reproduce this thesis by photocopying or by other means, in total or in part, at the request of other institutions or individuals for the purpose of scholarly research. I understand that my thesis will be made electronically available to the public.

Zainab Maqsood

STATEMENT OF CONTRIBUTIONS

I hereby certify that I am the sole author of this thesis and that no part of this thesis has been published or submitted for publication. I have used standard referencing practices to acknowledge ideas, research techniques, or other materials that belong to others.

ACKNOWLEDGEMENTS

I would like to express my gratitude towards to my supervisor Dr. Ying Wang for her continuous support, guidance and patience throughout my graduate studies. I would like to thank her for giving me this opportunity; without her this research and my post-graduate education would not have been possible. Also, I would like to thank both, Dr. Langis Roy and Dr. Ming Yu for sharing their knowledge. My sincere thanks to my colleagues and friends for their support. Lastly, I would like acknowledge my parents and husband for their love and support.

Zainab Maqsood

Oshawa, Ontario

February, 2021

TABLE OF CONTENTS

LIST OF TABLES

LIST OF FIGURES

LIST OF ABBREVIATIONS AND SYMBOLS

DRA	Dielectric Resonator Antenna
EM	Electromagnetic
5G	Fifth Generation
mm-wave	Millimeter-wave
Q	High-Quality
Q_{EXT}	External Quality Factor
SIW	Substrate Integrated Waveguide
FBW	Fractional Bandwidth
HFSS	High-Frequency Structural Simulator
CPU	Central Processing Unit
ADS	Advanced System Design
TE	Transverse Electric

Chapter 1

Introduction

1.1 Context

In the past several years, mobile radio and wireless communication technology has advanced rapidly due to an increased number of wireless broadband and multimedia users. In order to meet the requirements of high mobile and wireless traffic volume, significant research has been conducted on the next generation of wireless network, the fifth generation (5G). 5G promises to mediate the increased mobile and wireless communication traffic by providing 1000 times increased capacity, 10-100 times higher data-rate and support 10-100 times higher number of connected devices as compared to the existing 4G wireless networks [1]. The hardware requirements of realizing 5G are expected to be met by hardware operating at the new spectrum in the microwave bands, 3.3 GHz – 4.4 GHz, and millimeter-wave (mm-wave, 24 GHz – 80 GHz) bands [2]. A combination of microwave and mm-wave bands is important for 5G as lower frequencies (microwave band) can be used for wide area coverage, and the higher frequencies (mm-wave band) for local and personal area communications [3]. Considerable research efforts have been put into innovative designs for both microwave and millimeter wave frequency bands to meet new requirements and challenges. This thesis focuses on microwave circuits operating at microwave bands.

1.2 Thesis Motivation and Objectives

Microwave circuits can generally be realized in two types of technologies, planar and non-planar. Non-planar circuits include waveguides, for example rectangular waveguides, that are often used for high-quality (Q) factor and low loss applications. However air-filled waveguides are bulky, especially for low frequency applications, and difficult to integrate with other circuits. Planar circuits include, for example, microstrip circuits. These circuits are desirable for their low profile, ease of fabrication and low cost. However, the loss is typically higher. For both types of technologies, circuit size reduction can be obtained with the use of high dielectric constant substrate or filling material.

The availability of a high dielectric constant (approximately 20) and low loss material provides the opportunity to explore novel design techniques for miniaturizing microwave filters and antennas. Not only does a high dielectric constant lead to highly compact designs, but at the same time it limits the bandwidth and can be useful for filtering. The overall objective of this thesis is to investigate combinations of planar and non-planar circuits that achieve compact integration of microwave filters and antennas, and to study both the implementation methods and performance limitations of such designs.

Microwave antenna and filter circuits are key components in all types of wireless communication systems. In conventional communication systems, antennas and filters are typically designed separately and then combined via connectors/adapters and/or interconnecting transmission lines. The use of extra connectors and/or cables results in the introduction of additional loss and a degraded filtering antenna system performance. Therefore, in order to obtain a low loss filtering antenna system, a co-design approach can

be taken. For example, the antenna can be treated as a load for the filter. Or the integration can be implemented by replacing the last resonator of the filter with an antenna that has the same centre frequency as the filter.

Although research has been done on antenna and filter integration, most of it consists of studies on planar implementations, such as microstrip or slot antennas integrated with substrate integrated waveguide (SIW) filters. Also, many of these studies report single polarized filtering antennas; there are few dual-polarized filtering antenna designs, especially for dielectric resonator antennas (DRA). In this thesis, two different filtering antenna designs are presented. Microstrip and DRAs are used due to their low-profile, ease of fabrication and light weight. Both designs are compact, low loss, and have dual-polarization with good isolation, making them ideal for 5G mobile communication applications.

1.3 Thesis Contributions

This thesis has developed original, compact, high performance microwave filter-antenna designs using high dielectric constant material. The designs overcame high dielectric constant limitations which caused difficulties in implementation and limited bandwidth. Two different methods were proposed in this thesis to integrate microwave waveguide filters and antennas, with dual polarizations.

A dual-mode waveguide iris filter and microstrip antenna integration in the 3.5 – 3.7 GHz frequency range was first presented. Parametric analysis of the microstrip antenna allowed the impact of varying antenna dimensions on the integrated design to be studied. The filter-

antenna integration procedure was presented and discussed. The dual polarized microstrip filtering antenna design was simulated using a full wave electromagnetic (EM) simulator.

The dual-mode waveguide filter was then used for another antenna-filter integration design involving a DRA, again operating in the 3.5 – 3.7 GHz range. The impact of varying DRA dimensions on design parameters, including the external quality factor of the antenna, was studied. The design challenge and limitations caused by the high dielectric constant of the DRA were discussed. Similar to the microstrip filtering antenna design, filter-antenna integration was implemented using a full wave EM simulator, with the help of a circuit model.

Both structures achieved a dual polarized filtering response with a high isolation and gain. Also, both were implemented using materials with a high dielectric constant, resulting in highly compact designs with low insertion loss. To the best of our knowledge, such antenna-filter integrations have not been reported in the literature.

1.4 Thesis Outline

Chapter 1 provides an overview, motivation, and contributions of this thesis.

In chapter 2, recent developments on microstrip and dielectric resonator antennas, and dual-polarization designs are discussed. Research on various types of filter and antenna integration techniques, specifically techniques involving microstrip antennas and DRAs are reviewed.

In chapter 3, the theory and design of the dual-mode waveguide filter and dual polarized microstrip antenna are presented. A detailed description of the filter antenna integration procedure is then shown. EM simulation results of the microstrip filtering antenna structure are presented and discussed.

In chapter 4, the theory and design of the DRA are presented. The same waveguide filter shown in chapter 3 is used for the design of the filtering antenna structure displayed in chapter 4. The filter antenna integration procedure is shown, design challenges are discussed, and EM simulation results are presented.

In chapter 5, conclusions are drawn based on chapter 3 and 4. Future work is also discussed.

Chapter 2

Literature Review

In this chapter, research on different types of filter and antenna integration techniques, microstrip filtering antennas and dielectric resonator filtering antennas is reviewed. Recent developments with regards to microstrip and dielectric resonator antennas are also discussed.

2.1 Microstrip Antennas

In many applications involving aircraft, spacecraft, mobile radio and wireless communications systems where size and weight are constraints, low profile antennas may be required. A microstrip antenna is an ideal candidate for such applications as it is a low-profile antenna that is flexible enough to conform to both, planar and nonplanar surfaces, and is inexpensive to fabricate [4]. Typically, a microstrip antenna consists of two parallel conducting layers separated by a dielectric substrate. The lower conductor functions as a ground plane while the upper conductor is a thin metallic strip, also known as a patch [5]. A typical square patch antenna is shown in Figure 2.1. Various feeding configurations for microstrip antennas have been introduced. The most commonly used configurations include microstrip line, coaxial probe and aperture coupling [6]-[8].

Antenna parameters such as bandwidth and resonant frequency can be modified by adding loads between the patch and the ground plane. The bandwidth of a patch antenna can be improved by modifying the reverse bias across a varactor diode placed between the patch

and the ground plane [9]. Another method used to increase the antenna bandwidth includes stacking two radiating patches and/or substrates on top of each other as shown in [10]-[12]. Resonant frequency of the antenna can be modified by the placement of a shorting pin in between the two conductors of the antenna [13].

In comparison to other patch configurations, the rectangular microstrip antenna is most widely used due to its merits of lower manufacturing cost, simple design, ease of installation, low-profile and symmetry of structure. A minor disadvantage of rectangular patch antennas includes high levels of cross-polar radiation in the far-field in both, diagonal planes and in the H-plane. In the case of a dual-polarized antenna system, high levels of cross polar radiation would introduce a high chance of an error in transmission [14]. Various designs and analysis of the generic rectangular patch and recent advancement in the design/topologies of rectangular patch antennas are discussed in [15]-[23].

Dual-polarized antennas are ideal for 5G applications due to their ability of allowing the transmission/reception from both horizontal and vertical polarized signals, which in turn significantly improves overall wireless communication system performance. In this thesis, dual-polarized antennas are used.

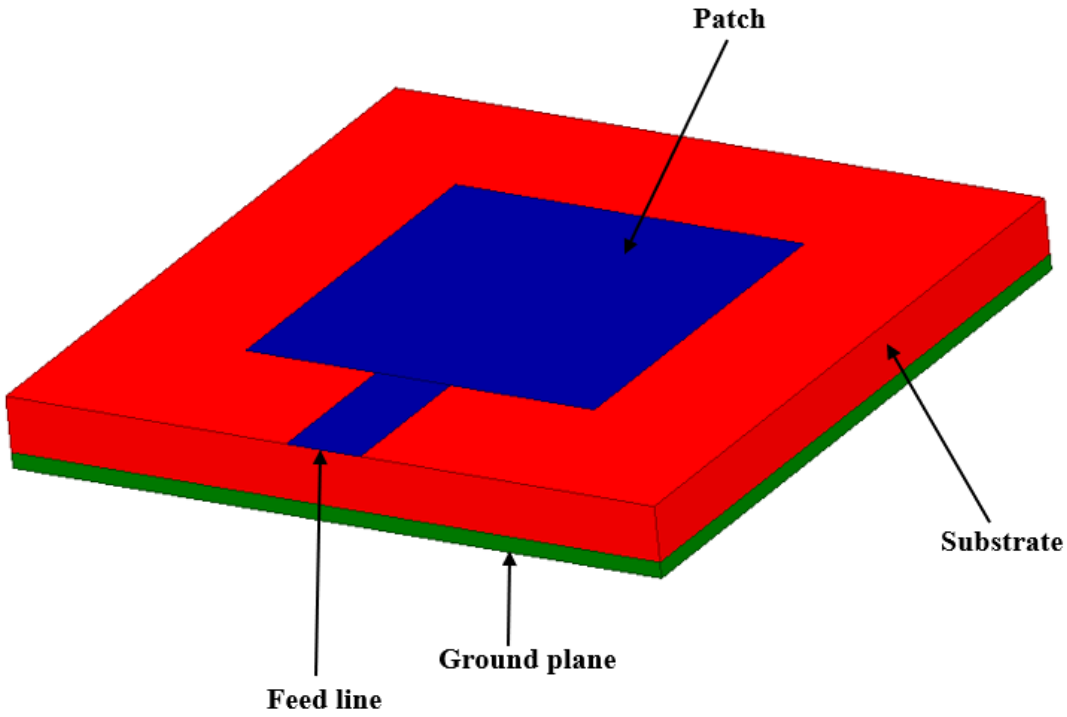

Figure 2.1: Square Patch Antenna Fed by Microstrip Line

2.2 Dielectric Resonator Antennas

The development of dielectric resonator antennas (DRAs) was followed by the introduction of dielectric resonators, which have been used as high-quality (Q) factor and compact elements in microwave circuit applications since the late 1960s [24]. In most cases, dielectric resonators are enclosed in metal cavities to maintain a high Q factor and to block radiation. Once the metal shield was removed from the dielectric resonator and an appropriate mode is excited in the resonator, it was observed that dielectric resonators are capable of becoming efficient antennas [25]. The first study of DRAs was conducted by Long, McAllister, and Shen in the 1980s [26]. Early studies of DRAs displayed characteristics of rectangular, cylindrical, and hemispherical shaped dielectric resonator

antennas [27], [28]. Rectangular shaped DRAs are commonly chosen out of the various DRA shapes due to its design simplicity and ease of fabrication [29].

A typical DRA sits on an infinite ground plane, has either a square, rectangular, cylindrical, hemicylindrical, or hemispherical shape, operates in a frequency of approximately 1 – 60 GHz, and has a dielectric constant (ε_r) within the range of 5 – 30 [30], [31]. A typical square DRA is shown in Figure 2.2. DRAs have many advantageous characteristics that allow them to be suitable for various applications including wireless communication systems, GPS, and satellite systems. Some of these characteristics include having a high radiation efficiency, large bandwidth, and a low profile [32]-[34]. Many feeding configurations for DRAs have been introduced. The most commonly used configurations include microstrip line [35], [36], aperture coupling [37]-[40], coaxial probe [41], [42] and rectangular waveguide excitation [43].

Over the last two decades, many significant contributions have been made to improve the design of DRAs. These improvements include different methods to increase antenna bandwidth since many existing and future wireless systems operate over wide frequency bands. Some of these methods involve DRAs in stacked configurations [44]-[46], modifications in the shape of DRAs [47]-[50] and combinations of DRAs with microstrip patches or monopoles [51]-[54].

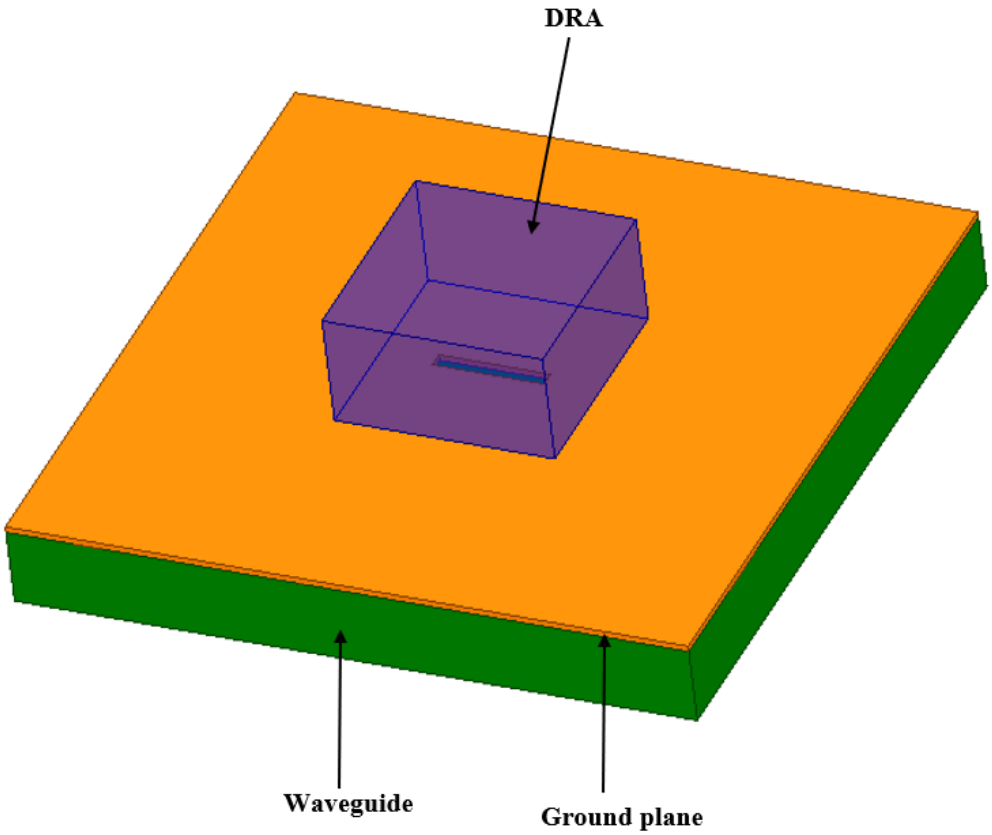

Figure 2.2: Square DRA Fed by Square Waveguide

2.3 Filter and Antenna Integration Techniques

Due to the rapid development of wireless communication and radar systems, more compact and highly efficient filters and antennas are in demand. High quality factor filters are key components for these systems due to their low insertion loss, which results in a significant improvement in the signal-to-noise ratio. This improvement directly enhances the sensitivity of communication/radar systems. Antennas also play a key role in improving the signal-to-noise ratio for receivers and minimize power consumption for transmitters [55]. In conventional systems, both, antennas and filters are designed separately and then

combined via, for example, coaxial cables. The usage of extra transmission lines results in the introduction of more loss and a degraded filtering antenna system performance [56]. Another method that can be used to connect a filter and an antenna is by the usage of slot-to-microstrip transition. This transition however, still introduces a significant loss to the filtering antenna system and degrades system performance due to the antenna loading effect [57]-[61].

A low loss filtering antenna system can be implemented by replacing the last resonator of a filter with an antenna that has the same centre frequency as the filter. For a successful integration, the last resonator of the filter and the antenna should have the same external quality factor (Q_{EXT}). Also, the internal coupling coefficient of the last resonator of the filter and the antenna to their preceding resonators should be identical. Once the conditions mentioned above are satisfied, the resulting filtering antenna will have a filtering response along with identical radiating characteristics as a typical standalone antenna [62]-[65]. In this thesis, the filtering antenna synthesis method is used to design both, the microstrip and dielectric resonator filtering antenna. Details on the implementation of this method are discussed in chapters 3 and 4.

2.3.1 Microstrip Filtering Antennas

There have been a number of reports on microstrip filtering antennas. In [66], the design with a second-order quasi-elliptic antenna gain response is presented. This structure is centered at 5 GHz and has a 2% fractional bandwidth. Mansour *et al.* presents third order bandpass filtering antenna with a centre frequency of 2 GHz [67]. Although good

simulation and measurement results are achieved for both designs, a detailed filter and antenna synthesis method is not given. In [68], a three pole bandpass filtering antenna with a centre frequency and fractional bandwidth of 10.27 GHz and 8.7%, respectively, is displayed. Li et al. presents second order bandpass filtering antenna with a fractional bandwidth of 2.5% and a gain of 6.85 dB [69]. These designs only consist of filtering antenna structures with a single polarization. For 5G applications, more efficient filtering antennas with dual-polarization are desired. In [70], a design of a dual-polarized quasi-elliptic bandpass filtering antenna with a centre frequency of 2.6 GHz and an isolation of 35 dB is shown. This structure, however, has a very narrow bandwidth of 100 MHz. In this thesis, a design of a dual polarized bandpass microstrip filtering antenna with a centre frequency of 3.6 GHz and a bandwidth of 200 MHz is presented.

2.3.2 Dielectric Resonator Filtering Antennas

There are limited number of reports on dielectric resonator filtering antennas. In [71], a dual-band filtering DRA with quasi-elliptic bandpass response is presented. The structure operates at 2.6 GHz with a bandwidth of 52.8%. A differential substrate integrated filtering DRA operating at 26 GHz with a 10.3% bandwidth is shown in [72]. Another substrate integrated waveguide filtering DRA is shown in [73]. This filtering antenna has a centre frequency of 35.5 GHZ and fractional bandwidth of 5.6%. All of these structures are for single polarization. Tang et al. presents a dual-polarized four-leaf-clover shaped filtering DRA with differential feeding ports. The structure operates at 2.6 GHz, with a bandwidth of 9.1% and 6.5dB gain [74]. This thesis aims at compact design that is easy to fabricate

and incorporates non-planar structure. As shown in chapter 4, a design of a dual polarized bandpass DR filtering antenna with a centre frequency of 3.6 GHz and a bandwidth of 200 MHz is presented.

Chapter 3 Microstrip Filtering Antenna

In this chapter, the theory and design of the dual-mode waveguide filter and dual polarized microstrip antenna are presented. This chapter starts with a detailed explanation of the design of the dual-mode waveguide filter and dual polarized microstrip antenna, respectively. The filter antenna integration procedure is then presented. A detailed description and implementation of the co-design approach via parameter extraction method is shown. Results of the microstrip filtering antenna structure are displayed and discussed.

3.1 Dual Mode Waveguide Filter

A three-pole dual-mode bandpass filter consisting of half-wavelength square cavity resonators is designed. Square cavities are selected for this design rather than the traditionally used rectangular cavities due to their symmetrical shape. A symmetrical cavity shape is required for the waveguide filter to achieve dual mode. Each square resonator operates in both, transverse electric TE_{011} and TE_{101} modes. The coupling between the cavities is achieved via irises, whereas the input/output coupling is realized with use of coaxial probes.

The filter is designed to have a centre frequency of 3.6 GHz with a bandwidth of 200 MHz. The following equation is used to calculate the cut-off frequency of the square waveguide [75]:

$$f_{cmn} = \frac{c}{2\pi\sqrt{\varepsilon_r}}\sqrt{\left(\frac{m\pi}{a}\right)^2 + \left(\frac{n\pi}{b}\right)^2} \qquad (3.1)$$

where *a* is the width of the waveguide, and *b* is the height of the waveguide. *m* represents the number of half-wavelength variations of electromagnetic (EM) fields in the "*a*" direction, *n* represents the number of half-wavelength variations of EM fields in the "*b*" direction, and *c* is the speed of light in vacuum. ε_r is the relative electrical permittivity of the dielectric material inside the waveguide. The waveguide is filled with a dielectric with ε_r = 20.

The fractional bandwidth (FBW) of the filter is calculated via the following equation [76]:

$$FBW = \frac{f_2 - f_1}{f_0} \tag{3.2}$$

where f_0 is the center frequency, and f_2 and f_1 define the passband of the bandpass filter.

The guided wavelength can be calculated using the following equations [76]:

$$\lambda_g = \frac{2\pi}{\beta} \tag{3.3}$$

$$\beta = \sqrt{\left(\frac{2\pi f_0 \sqrt{\varepsilon_r}}{c}\right)^2 - \left(\frac{\pi}{a}\right)^2} \tag{3.4}$$

where λ_g is the guided wavelength, and β is the propagation constant.

The prototype Chebyshev filter with the passband ripple L_{AR} = 0.04321 dB has the following element values [76]:

$g_0 = 1$

$g_1 = 0.8516$

$g_2 = 1.1032$

$g_3 = 0.8516$

$g_4 = 1$

Based on the element values above, the remaining filter design parameters can be calculated using the following equations [76]:

$$Q_{e1} = \frac{g_0 g_1}{FBW} \tag{3.3}$$

$$Q_{e3} = \frac{g_3 g_4}{FBW} \tag{3.4}$$

where Q_{e1} and Q_{e3} are the external quality factors of the filter at the input and output, respectively.

The input and output coupling of the filter is achieved via coaxial probe. The following equations can be used to calculate the characteristic impedance of cable, Z_0 [75]:

$$Z_0 = \sqrt{\frac{\mu_o \mu_r}{\varepsilon_0 \varepsilon_r} ln^2 \left(\frac{r_b}{r_a}\right)} \tag{3.5}$$

where r_a is the radius of the inner coax conductor, r_b is the radius of the outer coax conductor and Z_0 is the characteristic impedance of cable. The permittivity of free-space is represented by ε_0, μ_o is the permeability of free-space, μ_r is the relative permeability and ε_r is the relative permittivity of the dielectric for the coax cable. $\varepsilon_r = 2.08$ and $\mu_r = 1$ are assumed for the coax cable.

The coax cable input and output probe lengths are determined by use of the group delay method. This method determines the input/output coupling to a cavity resonator based on the group delay of the reflection coefficient S_{11}. The group delay of S_{11} (τ) is calculated based on the following equations [77]:

$$R = \frac{1}{g_0 g_1} \tag{3.6}$$

$$\tau = \frac{4}{2\pi BWR} \tag{3.7}$$

The EM simulator HFSS (High-Frequency Structural Simulator) is used to design the waveguide filter with dual polarization. HFSS calculates the EM fields of various high frequency electronic structures by using the finite element method. The 3D waveguide filter models with their respective parameter values are shown in Figures 3.1 – 3.3.

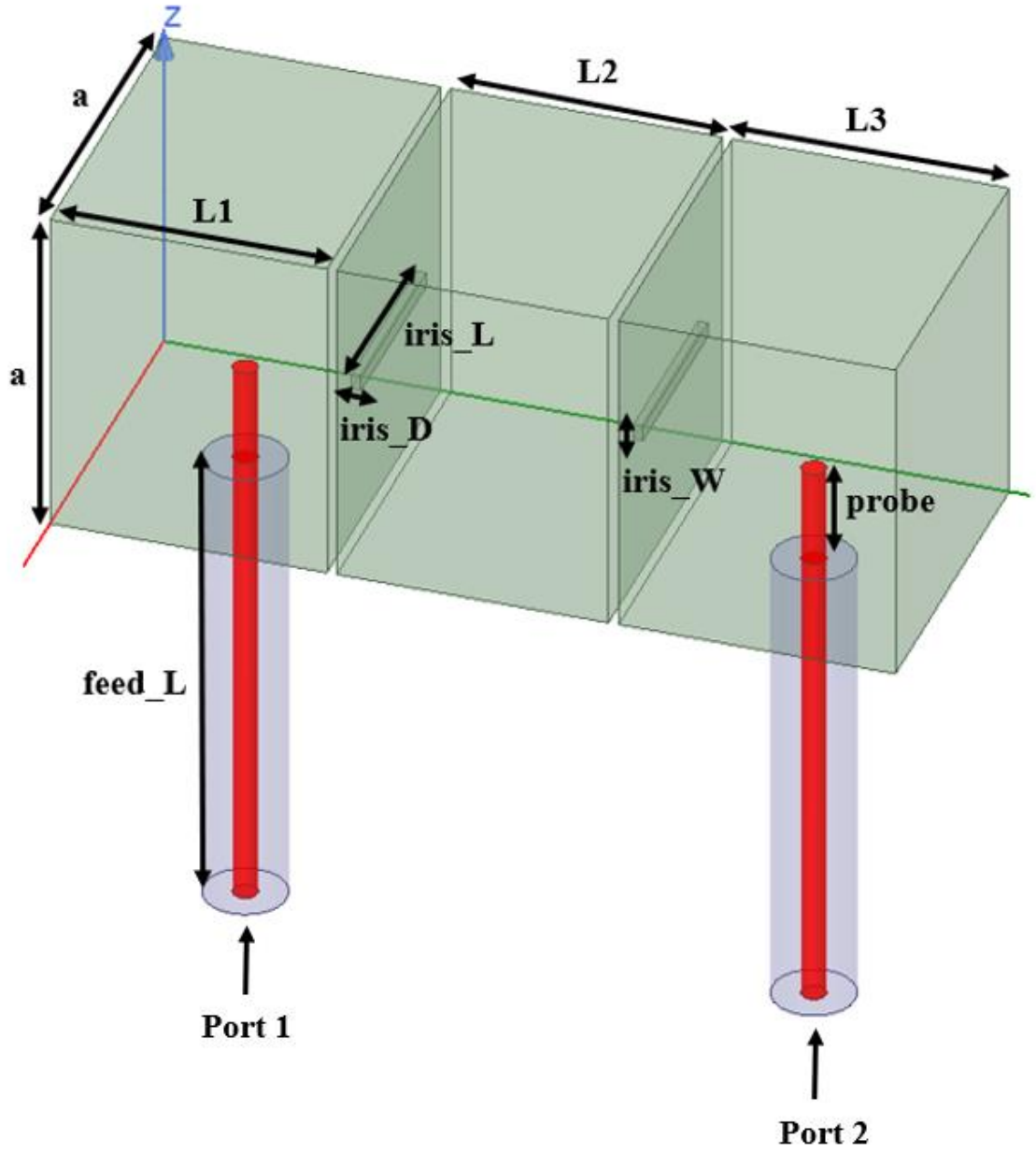

Figure 3.1: Waveguide Filter for TE_{101} Mode (a = 13.98 mm, L1 = 11.34 mm, L2 = 11.13 mm, L3 = 11.34 mm, iris_L = 7.97 mm, iris_D = 0.4064 mm, iris_W = 0.635 mm, probe = 4.16 mm, probe length =4.16mm, and feed_L = 20 mm)

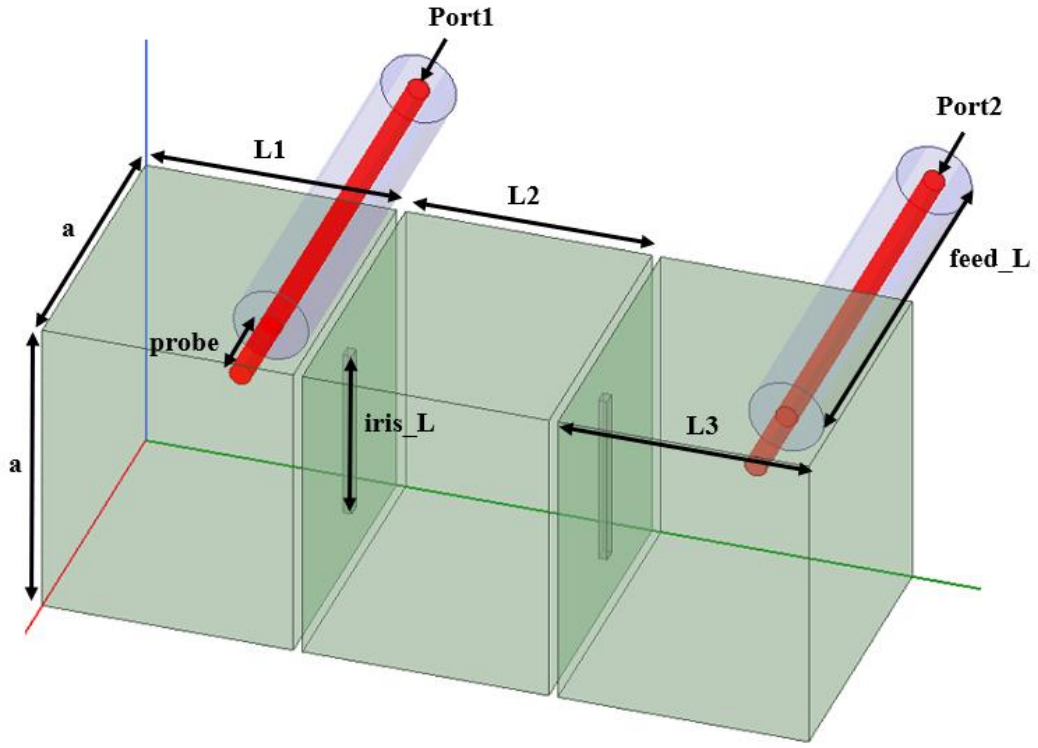

Figure 3.2: Waveguide Filter for TE_{011} Mode (a = 13.98 mm, L1 = 11.34 mm, L2 = 11.13 mm, L3 = 11.34 mm, iris_L = 7.99 mm, iris_D = 0.4064 mm, iris_W = 0.635 mm, probe = 4.16 mm, probe length =4.16mm, and feed_L = 20 mm)

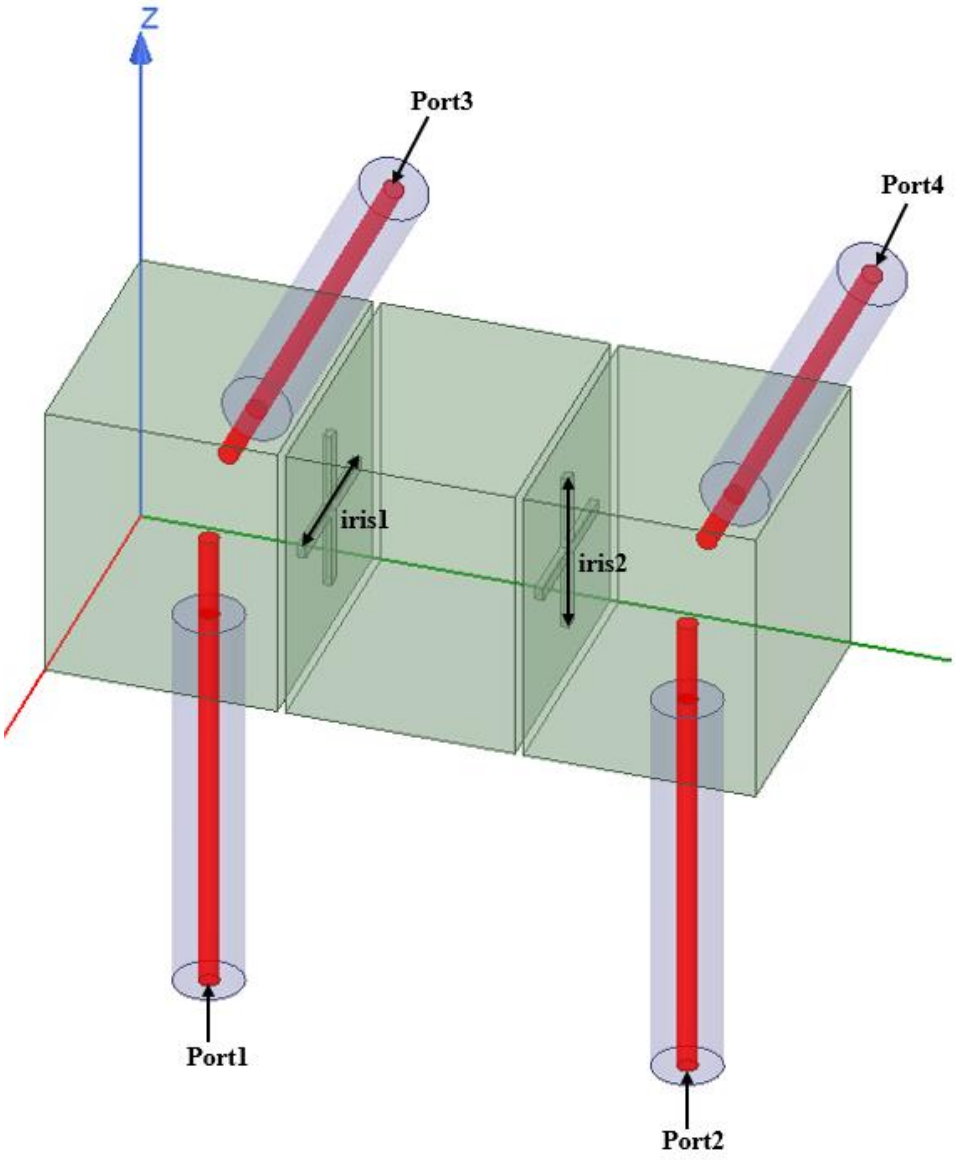

Figure 3.3: Waveguide Filter for TE_{101} and TE_{011} Modes (a = 13.98 mm, L1 = 11.31 mm, L2 = 11.15 mm, L3 = 11.31 mm, iris1 =8.02 mm, iris2 = 8.02 mm, iris_D = 0.4064 mm, iris_W = 0.635 mm, probe = 4.16mm, probe length =4.16mm, and feed_L = 20 mm)

The waveguide filter is optimized following the concept of the space mapping method. This method involves two models; one is called the "fine model" and the other is called the "coarse model". The fine model requires an excessive amount of central processing unit (CPU) time and produces very accurate results; while the coarse model requires significantly less CPU time and produces less accurate results. In this optimization

technique, the design parameter of the coarse model are assigned to the fine model for validation. After validation, if the design specifications are not met, the coarse model is updated via an iterative process involving parameter extraction.

The fine model of the waveguide filter is built using HFSS. The coarse model, also known as the equivalent circuit model, is built using the Keysight Advanced System Design (ADS) software. For the equivalent circuit model, the coupling between adjacent cavities is achieved via ideal impedance inverter, or *K* inverter. Within the ADS model space, the *K* inverter is represented by use of the ABCD matrix, and the half-wave cavities are modelled using the scattering parameters matrix. Also, all characteristic impedances are normalized to 1.

Equations to calculate the inverter impedance values are shown below [76]:

$$K_{01} = \sqrt{\frac{\pi\Delta}{2g_0g_1}} \tag{3.8}$$

$$K_{12} = \frac{\pi\Delta\lambda}{2\sqrt{g_1g_2}} \tag{3.9}$$

$$K_{23} = \frac{\pi\Delta}{2\sqrt{g_2g_3}} \tag{3.10}$$

$$K_{34} = \sqrt{\frac{\pi\Delta}{2g_3g_4}} \tag{3.11}$$

where K_{ij} represents impedance inverter values and Δ can be calculated using the equation below [76].

$$\Delta = \frac{\lambda_{g1} - \lambda_{g2}}{\lambda_{g0}} \tag{3.12}$$

where λ_{g0} is the guided wavelength at the centre frequency, λ_{g1} and λ_{g2} are wavelengths at the band edge frequencies of the bandpass filter.

Based on equations 3.3-3.4 and 3.9-3.12, the calculated Q_{EXT} and K-inverter impedance values are shown below:

$$Q_{EXT} = 15.32$$

$$K_{01} = 0.430$$

$$K_{12} = 0.163$$

$$K_{23} = 0.163$$

$$K_{34} = 0.430$$

The schematic of the equivalent circuit model is shown in Figure 3.4. The fine models built in HFSS are shown in Figure 3.1-3.3. The schematic of the coarse model represents the waveguide filter with a single polarization. Therefore, filters with single mode are tuned separately first, as shown in Figure 3.1 for TE_{101} mode and Figure 3.2 for TE_{011} mode, respectively. Filter tuning is performed via comparison of filter response from the coarse model with the filter response from the fine model. K-inverter values of the coarse model are extracted and compared with the ideal values. This method is used to optimize all cavity

and iris lengths. A comparison of fine and coarse model filtering response is shown in Figures 3.5 and 3.6. Fine tuning is needed when both modes are combined in the dual polarization design in Figure 3.3. The tuned filtering responses for the waveguide filter with dual-mode are shown in Figures 3.7-3.8. Based on the results shown in Figures 3.7-3.8, it can be seen that within the frequencies of 3.5-3.7 GHz, $|S_{11}|$ and $|S_{22}|$ of -20 dB and the isolation of -17 dB is achieved.

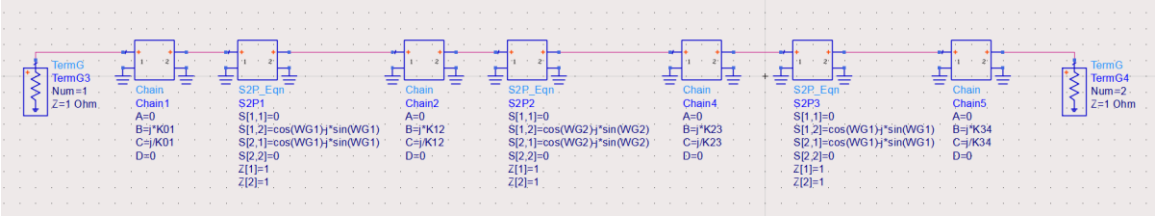

Figure 3.4: Filter Equivalent Circuit Model

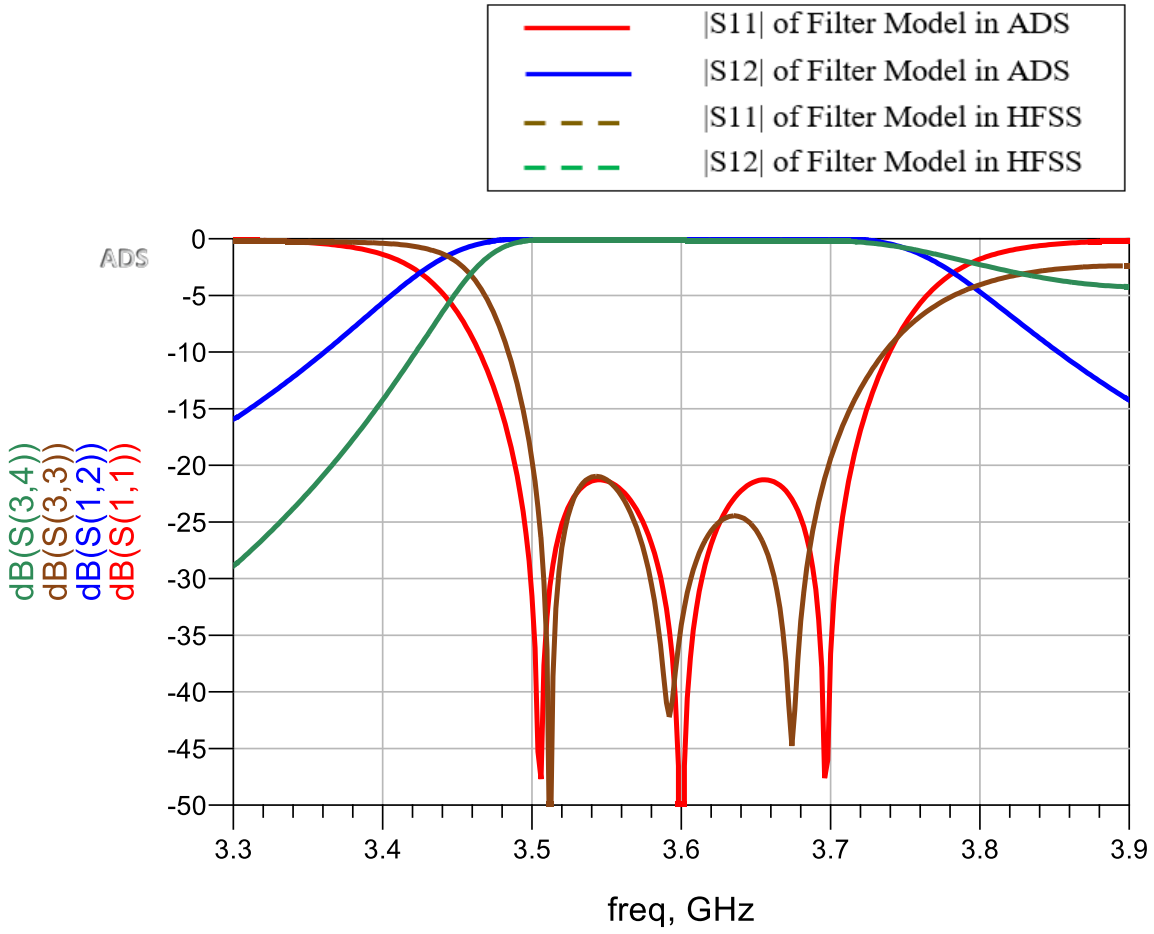

Figure 3.5: Waveguide Filter Response for TE_{101} Mode

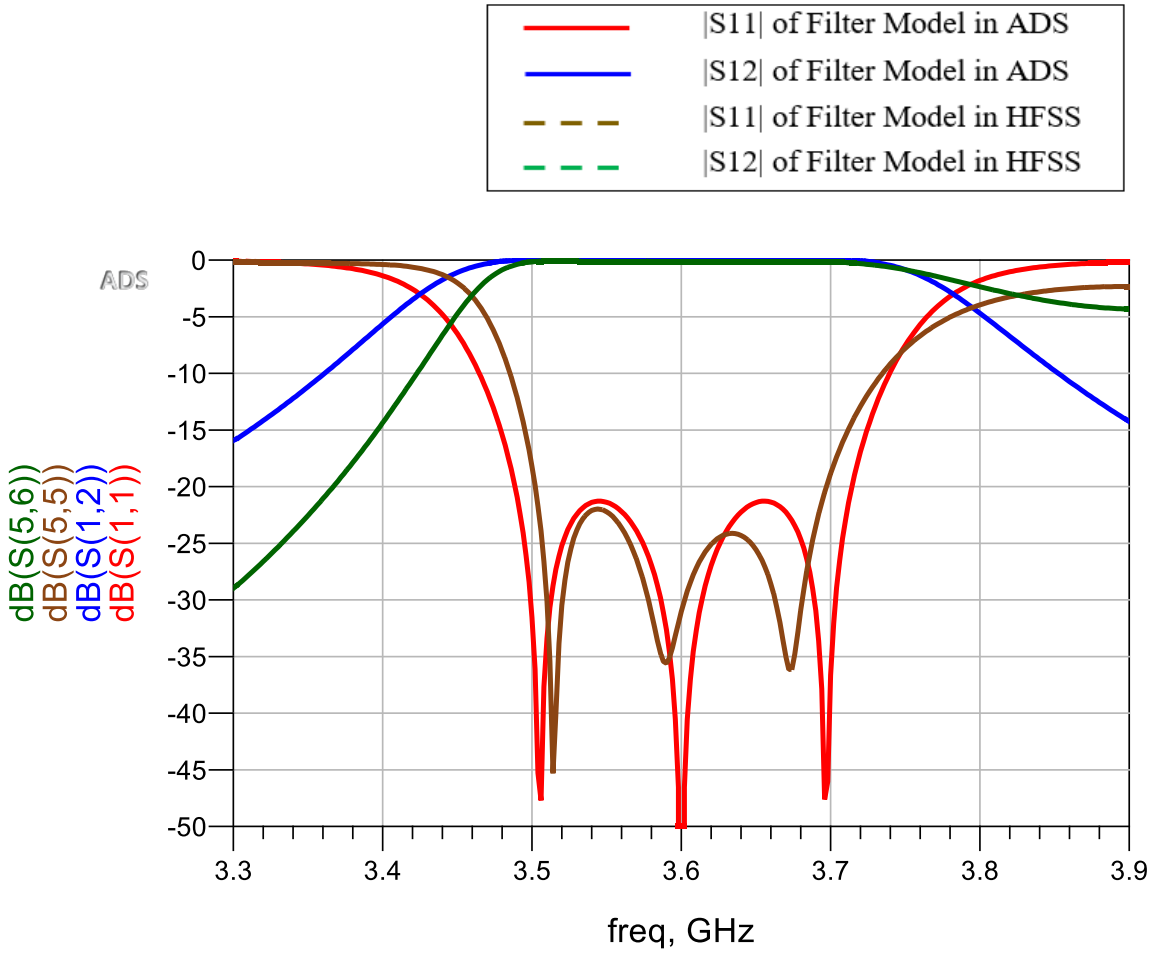

Figure 3.6: Waveguide Filter Response for TE_{011} Mode

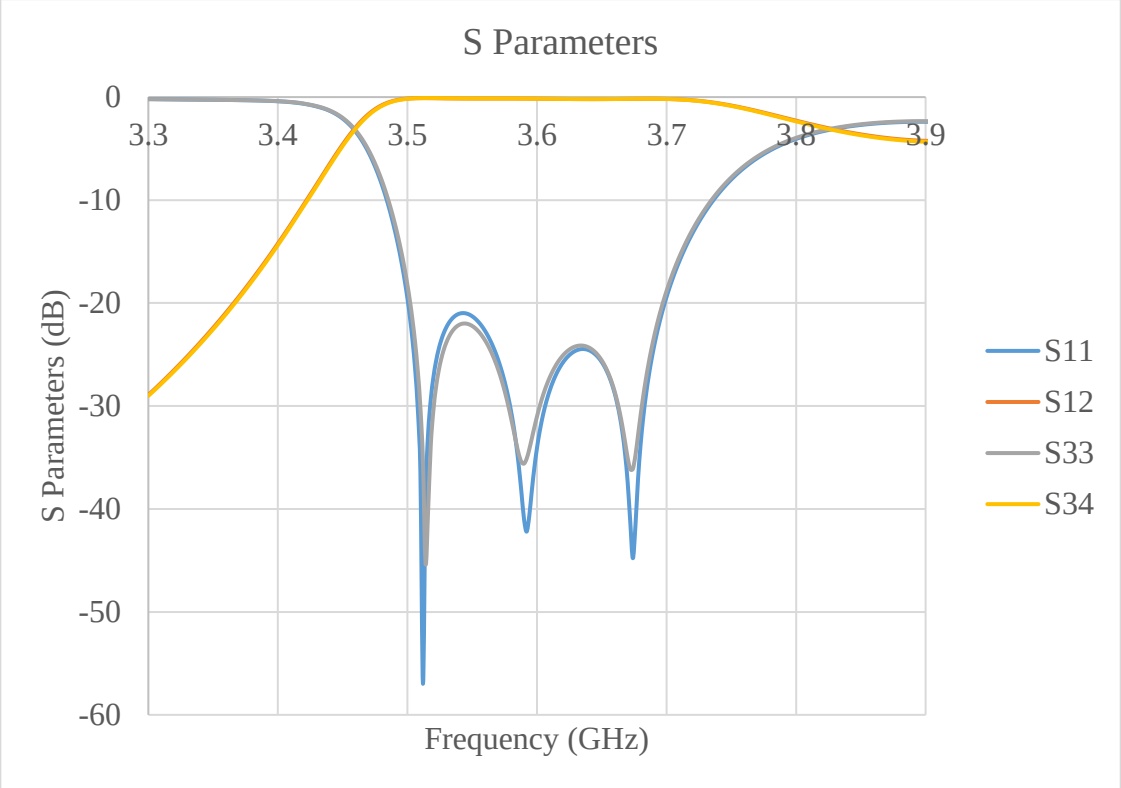

Figure 3.7: Optimized Response of Waveguide Filter With Dual Polarizations

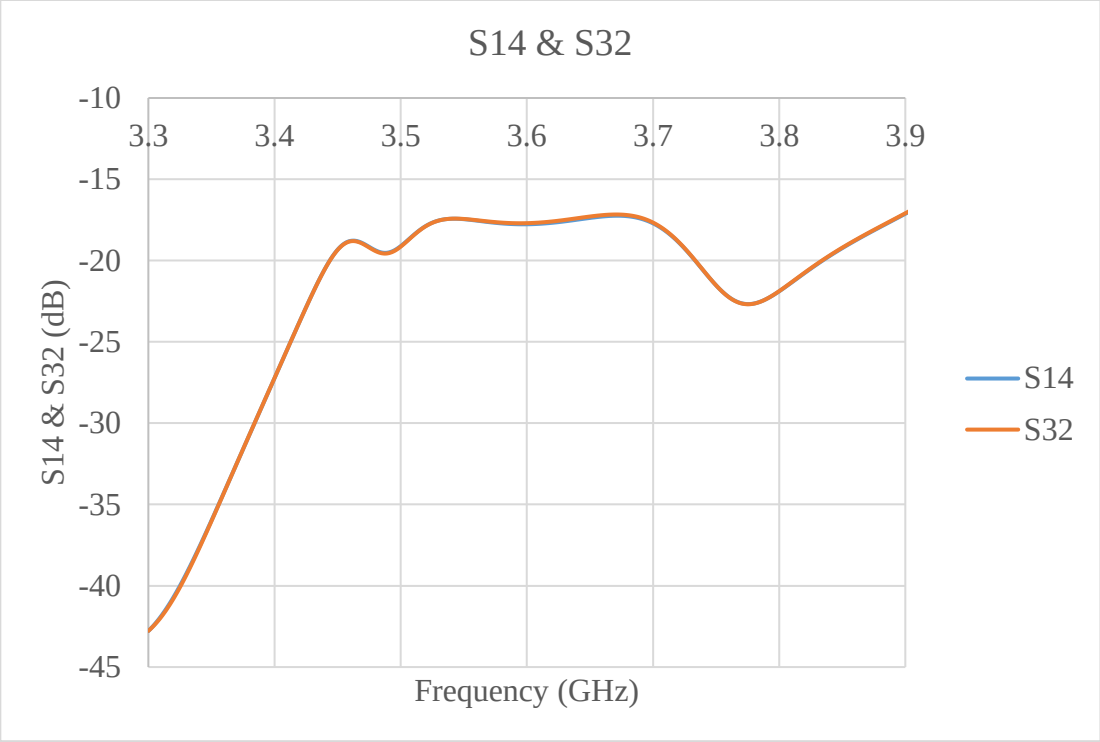

Figure 3.8: Isolation Between Ports of Waveguide Filter With Dual Polarizations

3.2 Filter Antenna Integration

Filter-antenna integration can be achieved by replacing the last resonator of the filter with an antenna possessing the same center frequency as the filter. A successful integration needs to satisfy the following two conditions [55]:

1. The last resonator of both the filter and the antenna have the same external quality factor (Q_{EXT}).
2. The internal coupling coefficient of both the last resonator of the filter and the antenna to their preceding resonators needs to be the same.

Once these conditions are met, the resulting filtering antenna will have a bandpass filtering response along with similar radiating characteristics as a typical standalone antenna.

In this thesis, two filtering antenna designs are presented:

1. Microstrip Filtering Antenna
2. Dielectric Resonator Filtering Antenna

In both cases, the antenna has the same bandwidth as the filter. This allows for the antenna to act as a resonator integrated to the filter. Detailed filter-antenna design methods and analysis for both microstrip and DR filtering antennas are presented in the remainder of this chapter and chapter 4, respectively.

3.3 Design of Microstrip Antenna

The microstrip antenna is a good candidate for 5G applications due to its flexible and low-profile structure, which is easy and inexpensive with respect to fabrication in comparison to other antennas. A patch with a square shape is selected and a waveguide with square cross-section is used to excite the antenna. The horizontal and vertical slots are used to excite the two polarizations respectively. The antenna is designed to operate at 3.6 GHz; the same frequency as the filter centre frequency. A Duroid substrate with dielectric constant (ε_r) = 2.2 and loss tangent tanδ = 0.0009 is used to design the antenna. The following equation is used to calculate the length/width of the patch [4]:

$$W = \frac{1}{2f_0\sqrt{\mu_0\varepsilon_0}}\sqrt{\frac{2}{\varepsilon_r + 1}} \tag{3.13}$$

where f_0 is the centre frequency of the antenna. The 3D model of the microstrip antenna is shown in Figure 3.9.

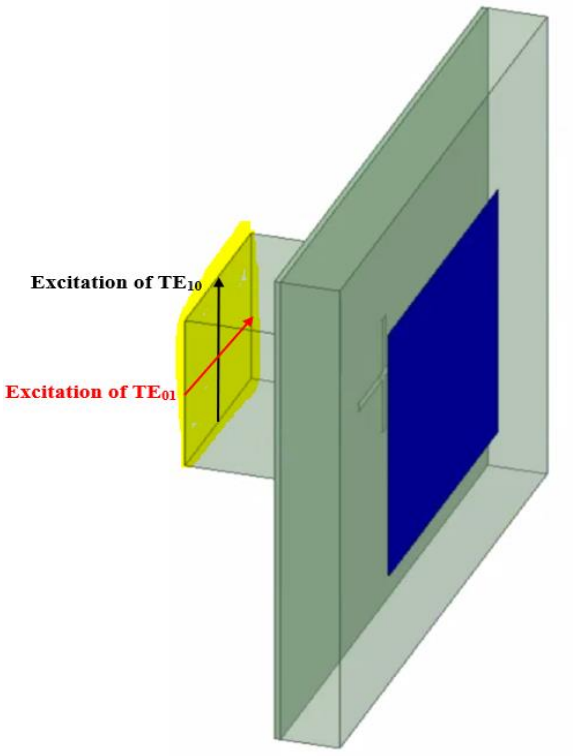

(a) Isometric View

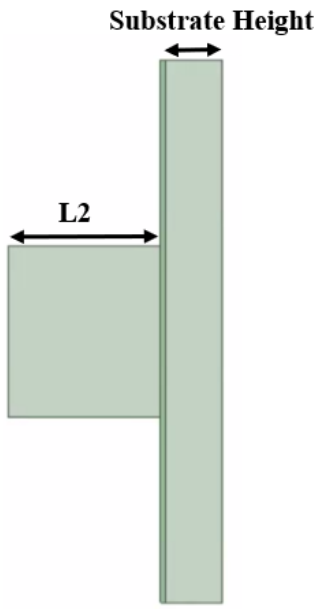

(b) Front View

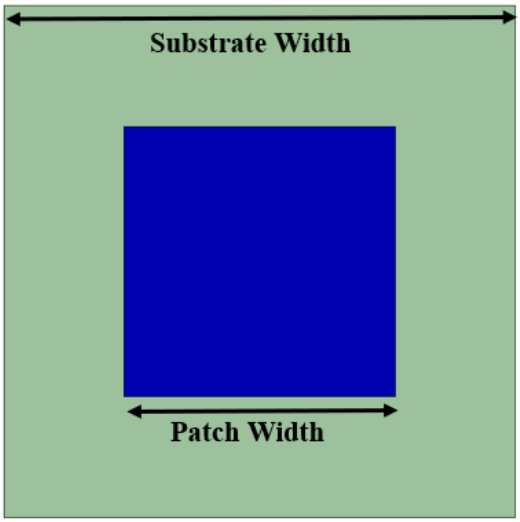

(c) Right Side View

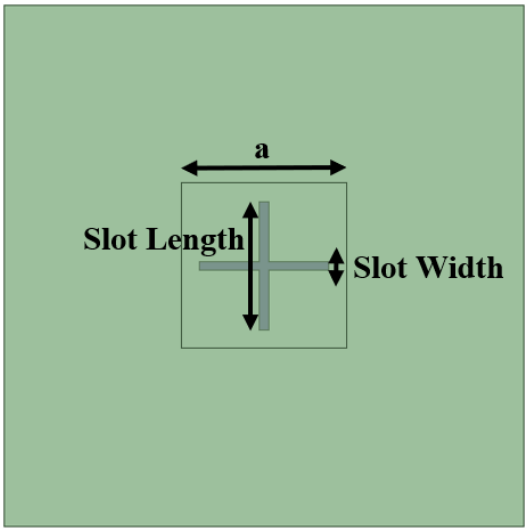

(d) Left Side View

Figure 3.9: Microstrip Antenna Model (a) Isometric View (b) Front Side View (c) Right Side View (d) Left Side View

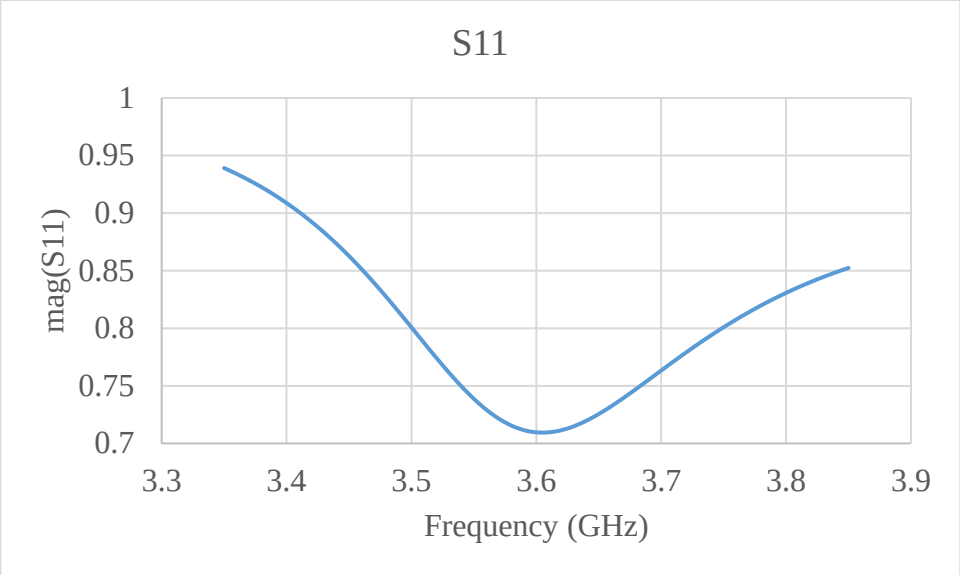

Figure 3.10: S_{11} Response of Microstrip Antenna

3.4 Extraction of Q_{EXT} of Antenna and Coupling between Antenna and Filter

An example of the S_{11} response when TE_{101} mode is excited is shown in Figure 3.10, which can be used to determine the bandwidth of the patch antenna. Q_{EXT} of the antenna is related to the bandwidth as shown below [55].

$$Q_{EXT} = \frac{f_0}{Bandwidth} \tag{3.14}$$

The following equation is used to determine the Q_{EXT} [52]:

$$\frac{1}{Q_{EXT}} = \frac{1}{Q_L} - \frac{1}{Q_U} \tag{3.15}$$

where Q_L is the loaded quality factor and Q_U represents the unloaded quality factor. If the antenna is assumed lossless, Q_U is infinitely large. Therefore,

$$\frac{1}{Q_{EXT}} = \frac{1}{Q_L} \tag{3.16}$$

The loaded quality factor can be determined from the analysis of the reflection coefficients of the antenna shown in Figure 3.10. As illustrated in Figure 3.10, S_{11}^{min} is the minimum reflection coefficient at the resonant frequency (f_0), f_1 and f_2 correspond to the frequencies when $|S_{11}| = S_{11}^{\Phi}$, where S_{11}^{Φ} can be calculated using the following equation [52]:

$$S_{11}^{\Phi} = \sqrt{\frac{1 + |S_{11}^{min}|^2}{2}} \tag{3.17}$$

As an example, based on equation above and S_{11} response of the microstrip antenna, the following values are calculated:

S_{11}^{min}= 0.7

f_0 = 3.6 GHz

f_1 = 3.48 GHz

f_2 = 3.76 GHz

S_{11}^{Φ} = 0.86

The coupling coefficient, *k*, between the input port and the resonator can be calculated using the following equations [52]:

$$k = \frac{1 - S_{11}^{min}}{1 + S_{11}^{min}} \quad \text{(resonator is undercoupled)} \tag{3.18}$$

$$k = \frac{1 + S_{11}^{min}}{1 - S_{11}^{min}} \quad \text{(resonator is overcoupled)} \tag{3.19}$$

Q_L can be calculated using the following the equation [52]:

$$Q_L = (1 + k)\frac{f_0}{f_2 - f_1} \tag{3.20}$$

In the following, equations (3.18) and (3.20) are used to calculate K_{23} and the external quality factor.

3.4 Parametric Study for Microstrip Filter Antenna Integration

Antenna design parameters such as slot length, slot width, and substrate height affect the coupling between antenna and the preceding filter resonator (K_{23}) as well as the antenna Q_{EXT}. The impact of varying substrate heights on Q_{EXT} and K_{23} is shown in Figures 3.11 and 3.12, respectively. A parametric analysis of both, slot length and slot width is carried out in three cases. In the first case, a slot width of 0.588 mm is selected and the impact of varying slot lengths on K_{23} and Q_{EXT} is studied. The analysis is shown in Figures 3.13 and 3.14. In the second case, a slot width of 0.688 is selected and again, the impact of varying slot lengths is studied; the results are displayed in Figures 3.15 and 3.16. In the last case, a slot width of 0.788 is selected and the results from changing slot lengths are shown in Figures 3.17 and 3.18.

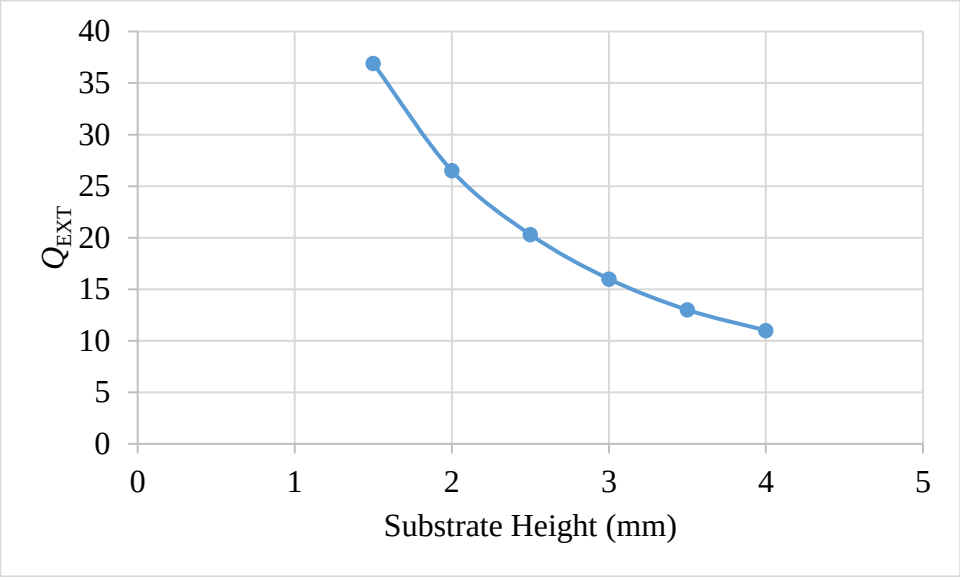

Figure 3.11: The impact of substrate height variation on Q_{EXT}, where slot length = 10.864 mm and slot width = 0.788 mm

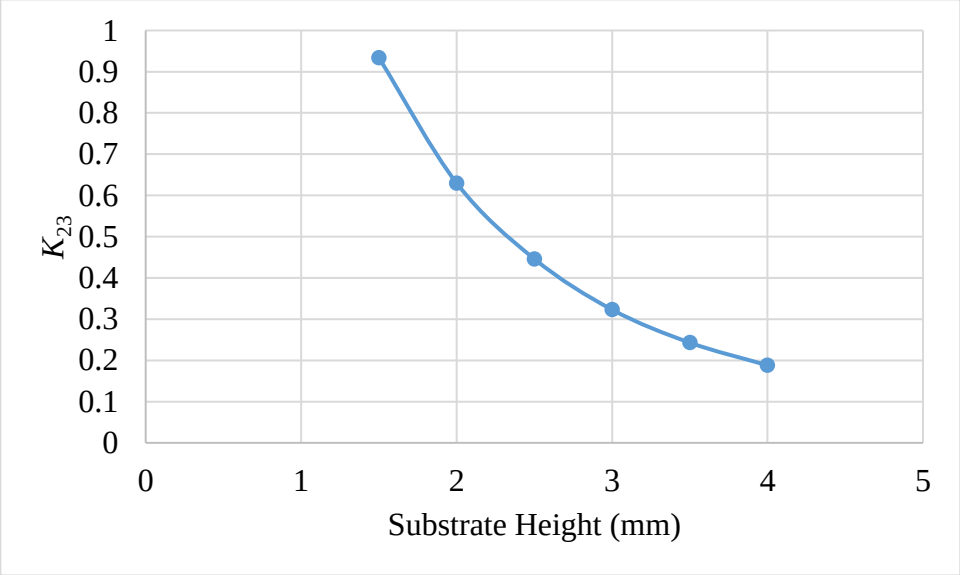

Figure 3.12: The impact of substrate height variation on K_{23}, where slot length = 10.864 mm and slot width = 0.788 mm

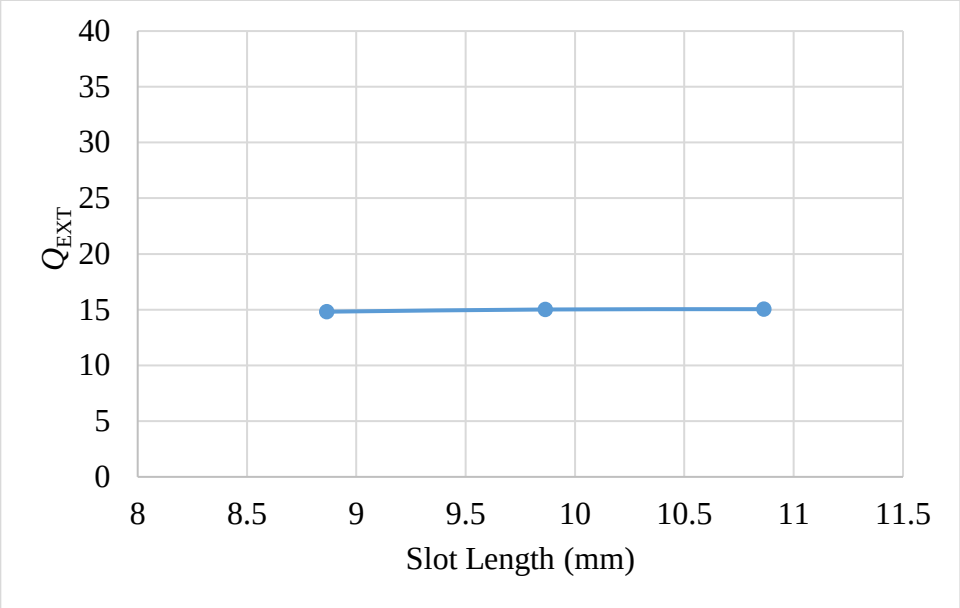

Figure 3.13: The impact of slot length variation on Q_{EXT}, where slot width = 0.588 mm and substrate height = 3.1 mm

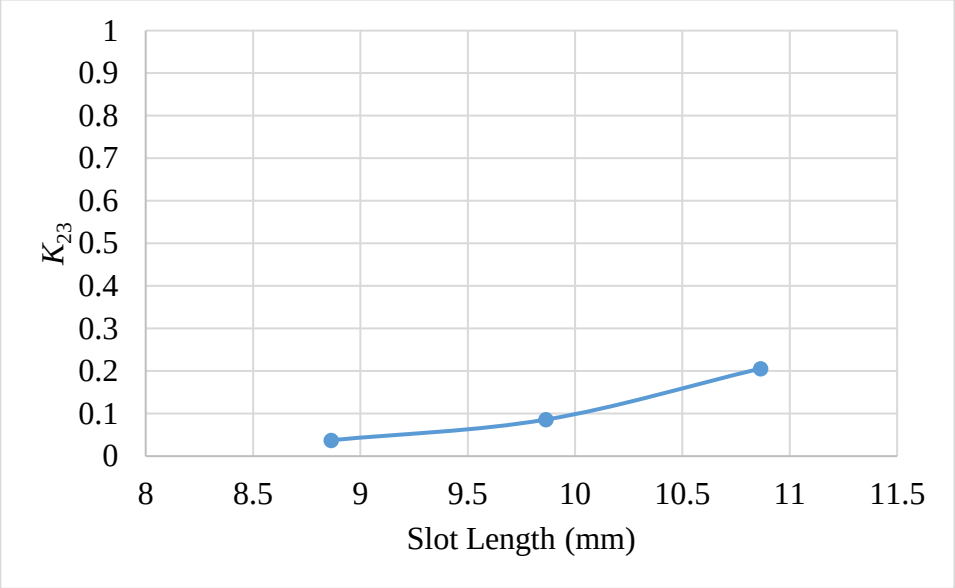

Figure 3.14: The impact of slot length variation on K_{23}, where slot width = 0.588 mm and substrate height = 3.1 mm

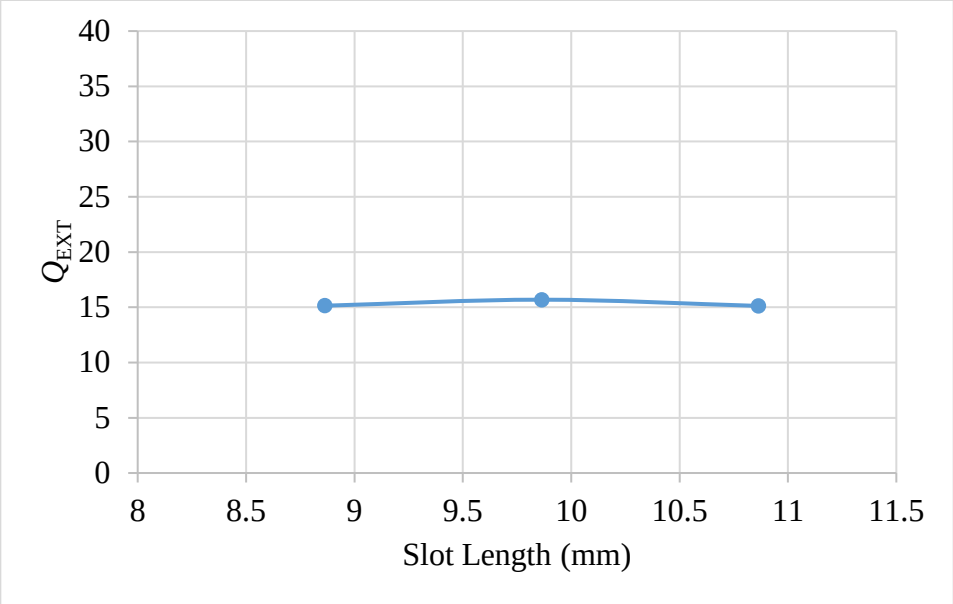

Figure 3.15: The impact of slot length variation on Q_{EXT}, where slot width = 0.688 mm and substrate height = 3.1 mm

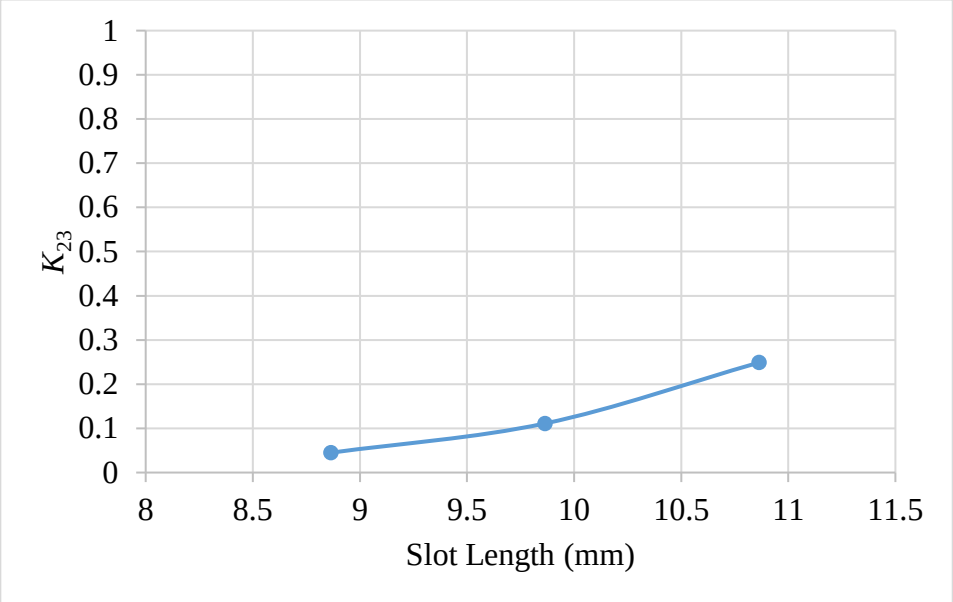

Figure 3.16: The impact of slot length variation on K_{23}, where slot width = 0.688 mm and substrate height = 3.1 mm

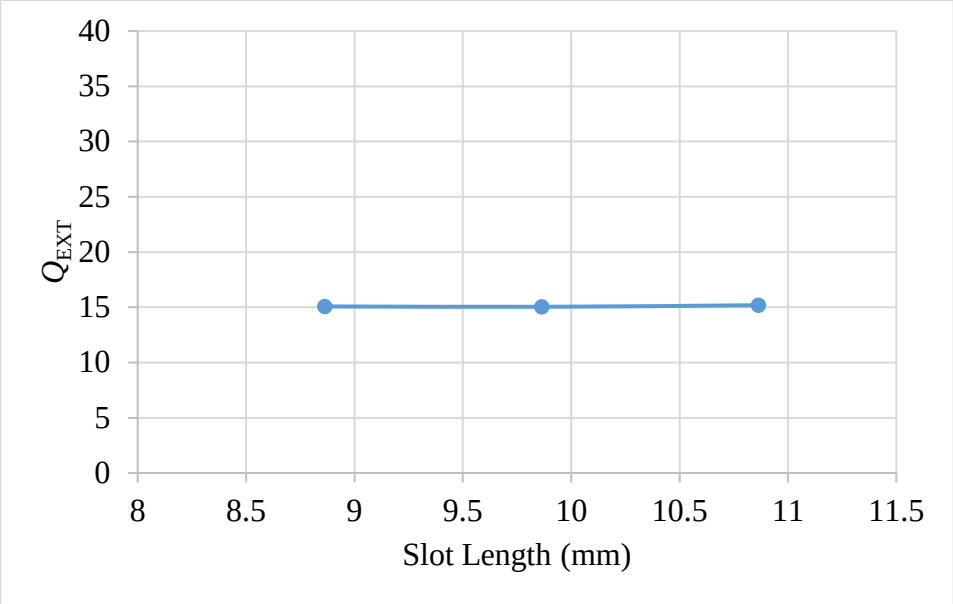

Figure 3.17: The impact of slot length variation on Q_{EXT}, where slot width = 0.788 mm and substrate height = 3.1 mm

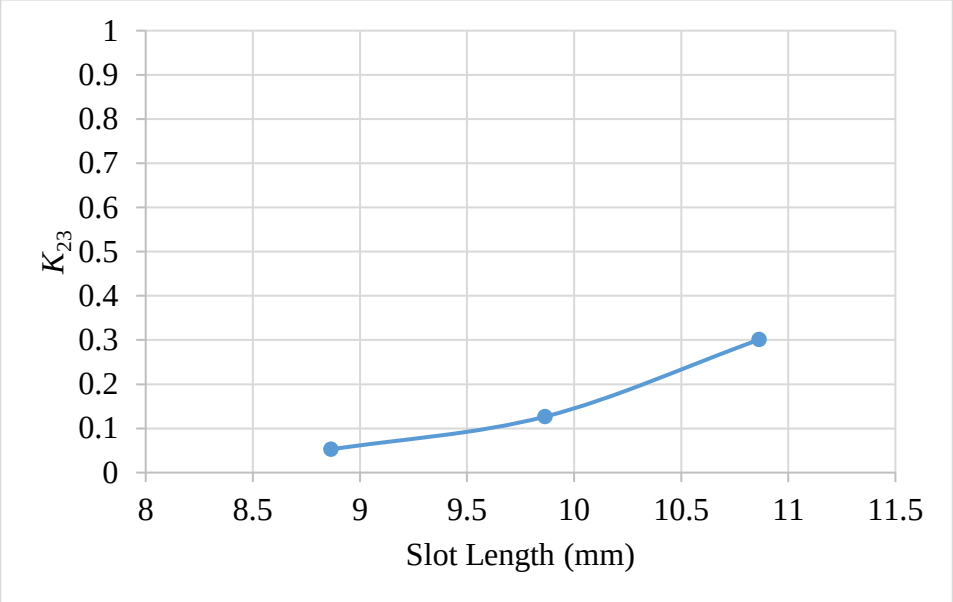

Figure 3.18: The impact of slot length variation on K_{23}, where slot width = 0.788 mm and substrate height = 3.1 mm

Based on the figures shown above, it is observed that as the substrate height increases, Q_{EXT} and K_{23} decreases. Another pattern that is deduced from the parametric analysis is that as the slot length increases, the K_{23} increases. The Q_{EXT}, however, does not chance much with varying slot lengths.

For a successful filter-antenna integration, the antenna should have similar Q_{EXT} as the filter and the coupling between the antenna and the filter should be close to K_{23} of the filter. Based on the Q_{EXT} and K_{23} of the filter in section 3.1 of this chapter (Q_{EXT} =15.32 and k_{23} = 0.163), the dimensions shown in Table 3.1 are selected for the microstrip antenna.

For comparison, ADS is used to model the last resonator of the filter; the schematic of the equivalent circuit model is shown in Figure 3.19. The patch antenna and last filter resonator $|S_{11}|$ responses are compared in Figure 3.20, showing good agreement. The Q_{EXT} and K_{23} of the patch antenna is 15.05 and 0.181, respectively.

The radiation patterns for both, E-plane and H-plane are displayed in Figures 3.21 and 3.22, respectively. Due to the symmetric nature of this antenna, the $|S_{11}|$ responses and radiation patterns are similar for both polarizations. For this reason, the results of the antenna for the case when TE_{101} mode is excited in the waveguide are only shown. Later in this chapter, the complete dual-polarized microstrip filtering antenna model and results for both polarizations are displayed.

Table 3-1: Microstrip Antenna Dimensions

Parameter	**Value**
a	13.98 mm
L2	11.34 mm
Substrate Height	3.1 mm
Substrate Width	43.94 mm
Patch Width	23.98 mm
Slot Length	10.264 mm
Slot Width	0.788 mm

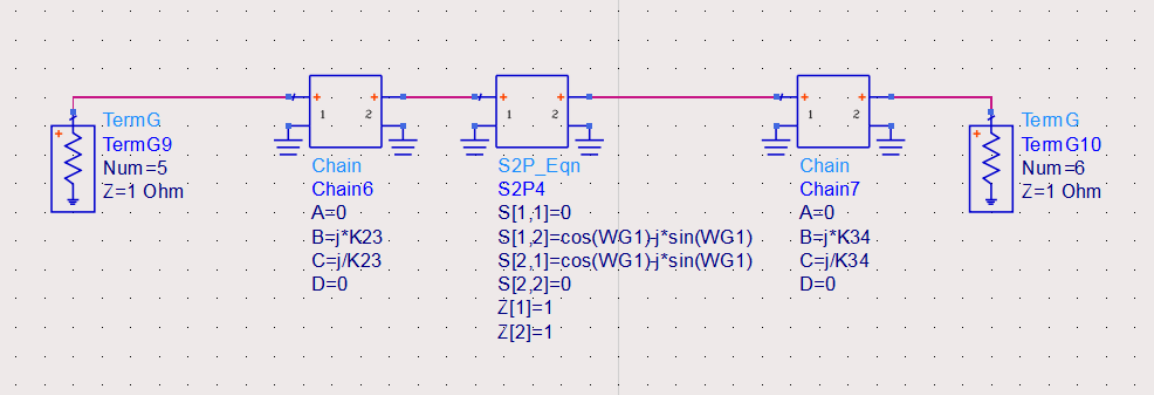

Figure 3.19: Last Filter Resonator Equivalent Circuit Model

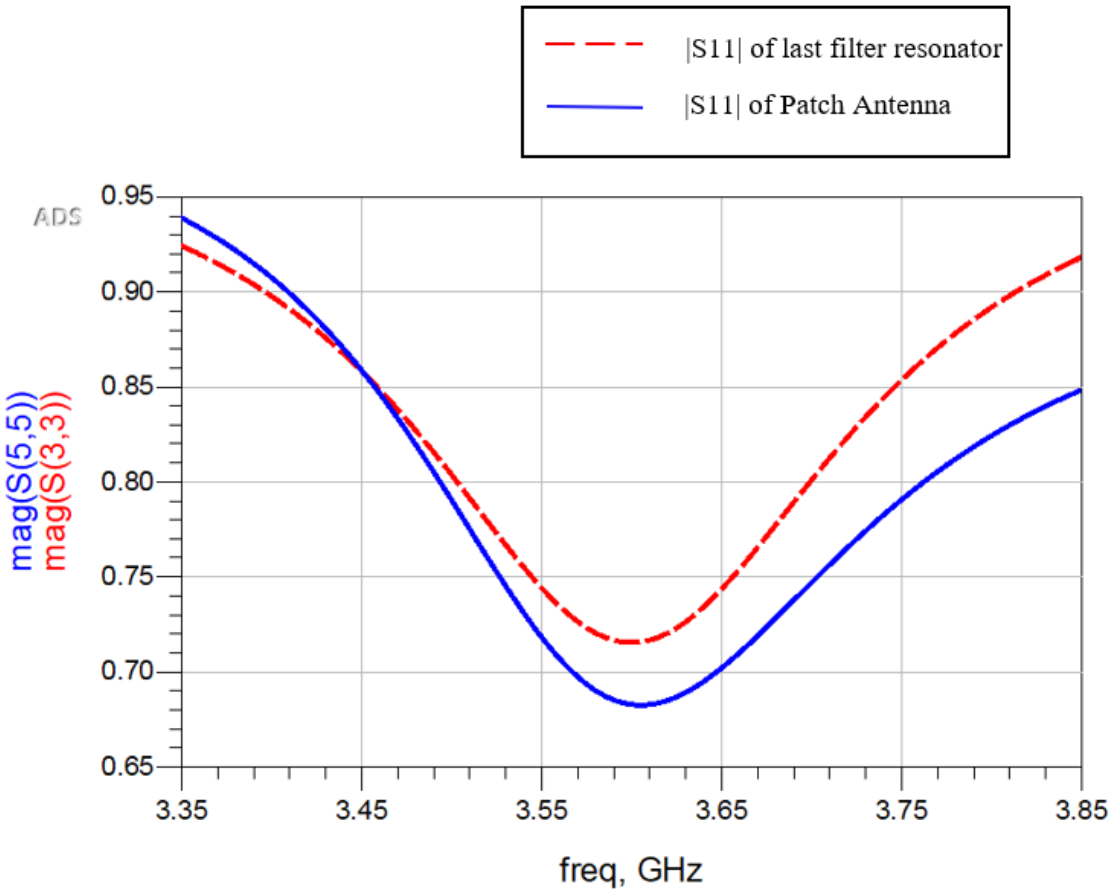

Figure 3.20: |S11| Response of the Patch Antenna and Last Filter Resonator

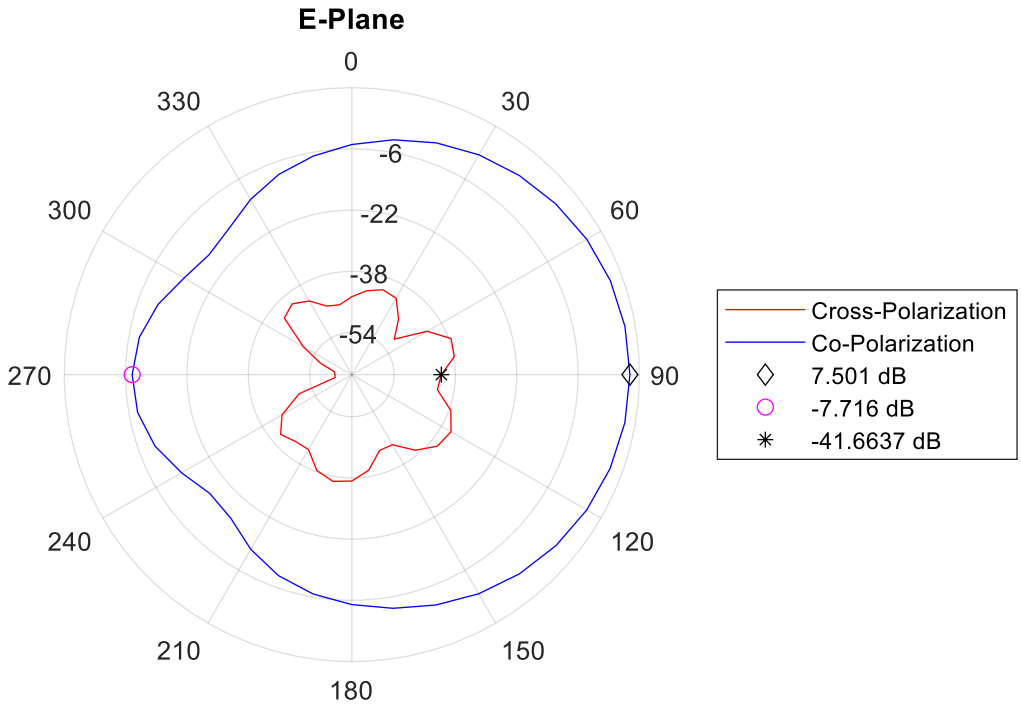

Figure 3.21: Microstrip Antenna Radiation Pattern E-Plane

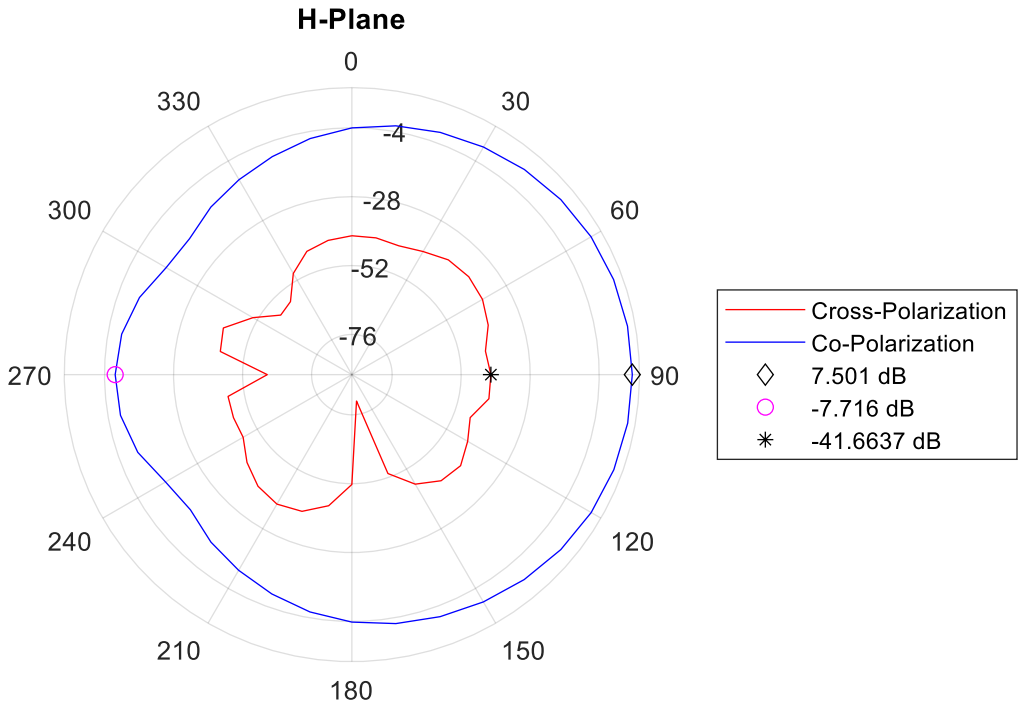

Figure 3.22: Microstrip Antenna Radiation Pattern H-Plane

3.5 Microstrip Filtering Antenna Simulation Results

The last step of the microstrip filtering antenna design process involves the replacement of the last filter resonator with the patch antenna. The dual polarized microstrip filtering antenna model is shown in Figure 3.23. Waveguide length L2 is adjusted in this step. All of the dimensions of this structure are displayed in Table 3.2. Figures 3.24 – 3.31 display results and various characteristics of this structure.

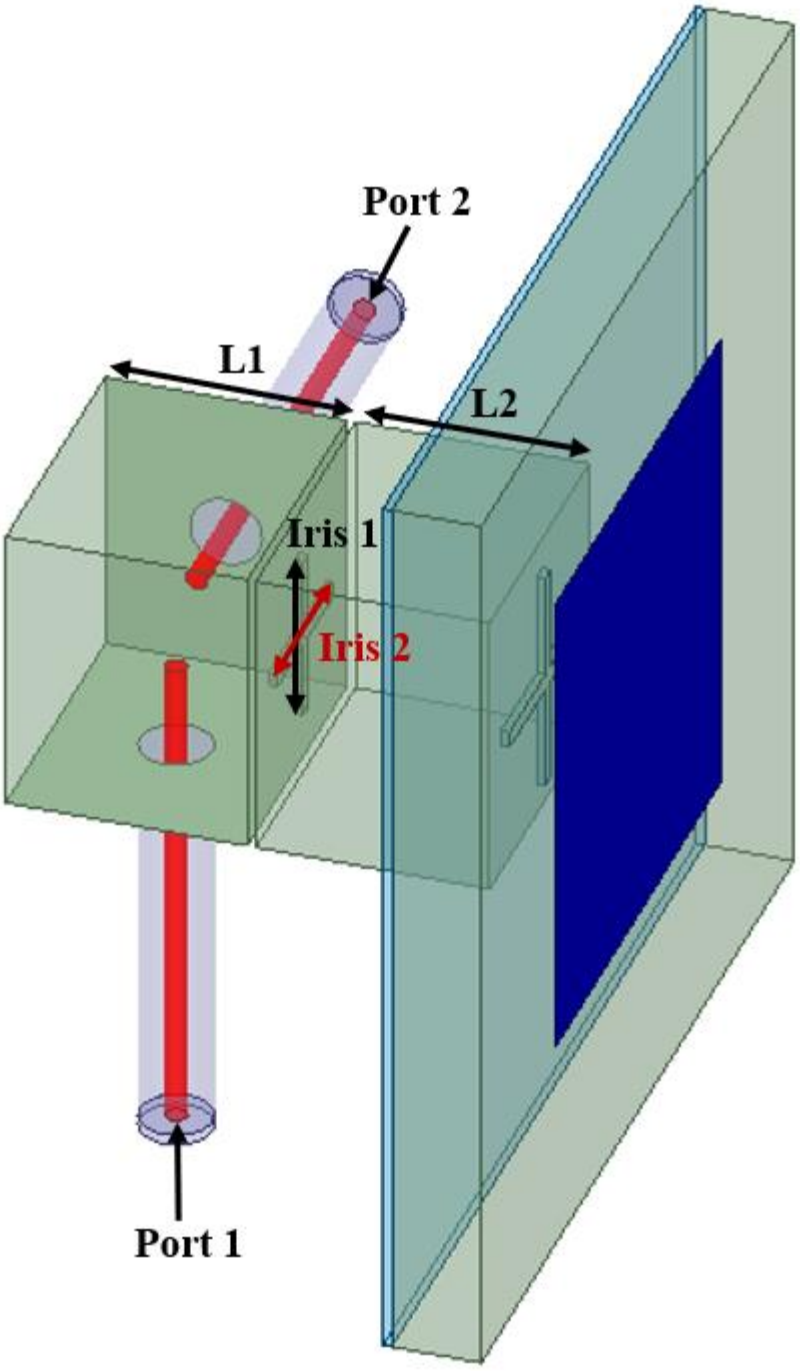

Figure 3.23: Microstrip Filtering Antenna Model

Table 3-2: Microstrip Filtering Antenna Dimensions

Parameter	**Value**
a	13.98 mm
L1	11.31 mm
L2	11.1 mm
Iris 1	8.02 mm
Iris 2	8.02 mm
iris_W	0.635 mm
Iris_D	0.4064 mm
Slot Length	10.264 mm
Slot Width	0.788 mm
Substrate Height	3.1 mm
Substrate Width	43.94 mm
Patch Width	23.98 mm
probe	4.15 mm

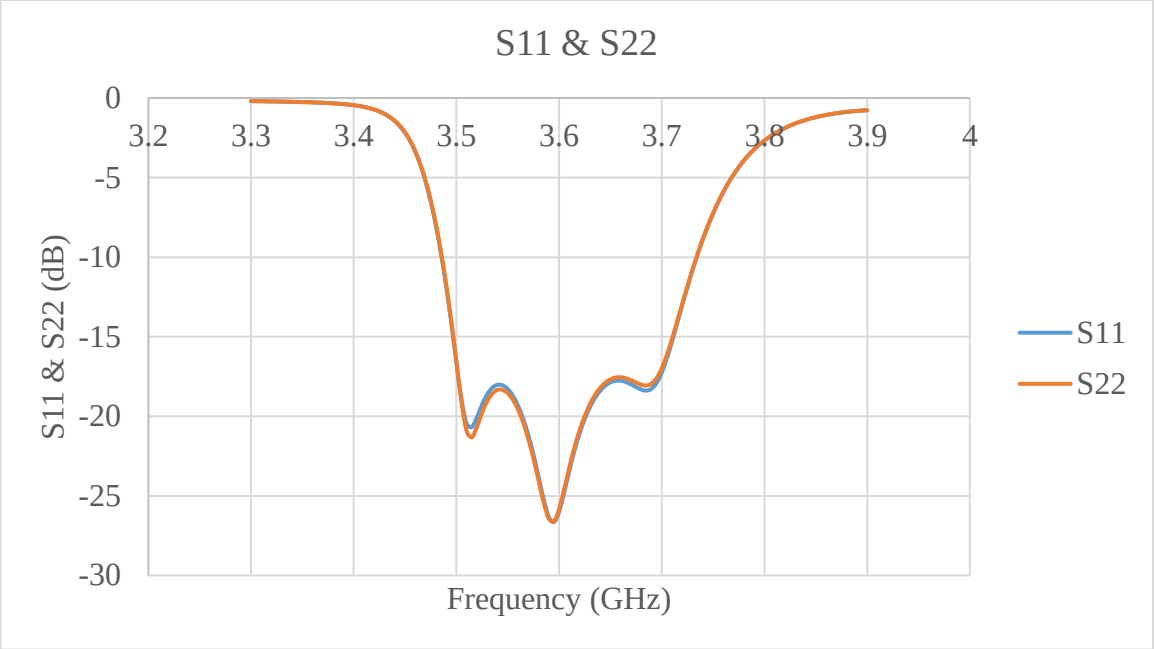

Figure 3.24: Microstrip Filtering Antenna S_{11} and S_{22} Responses

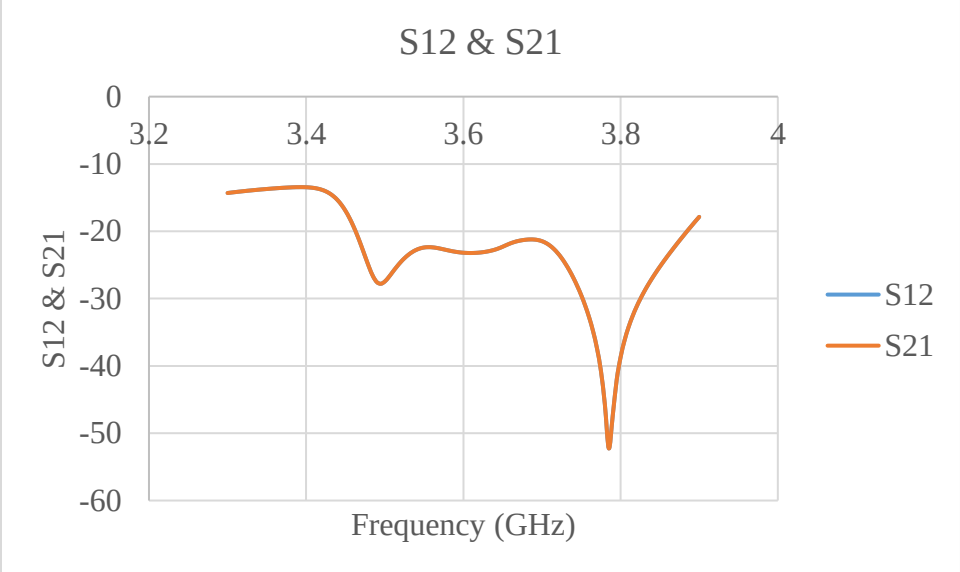

Figure 3.25: Microstrip Filtering Antenna S21 & S12 Response

Filtering Antenna Characteristics When Port 1 is Excited:

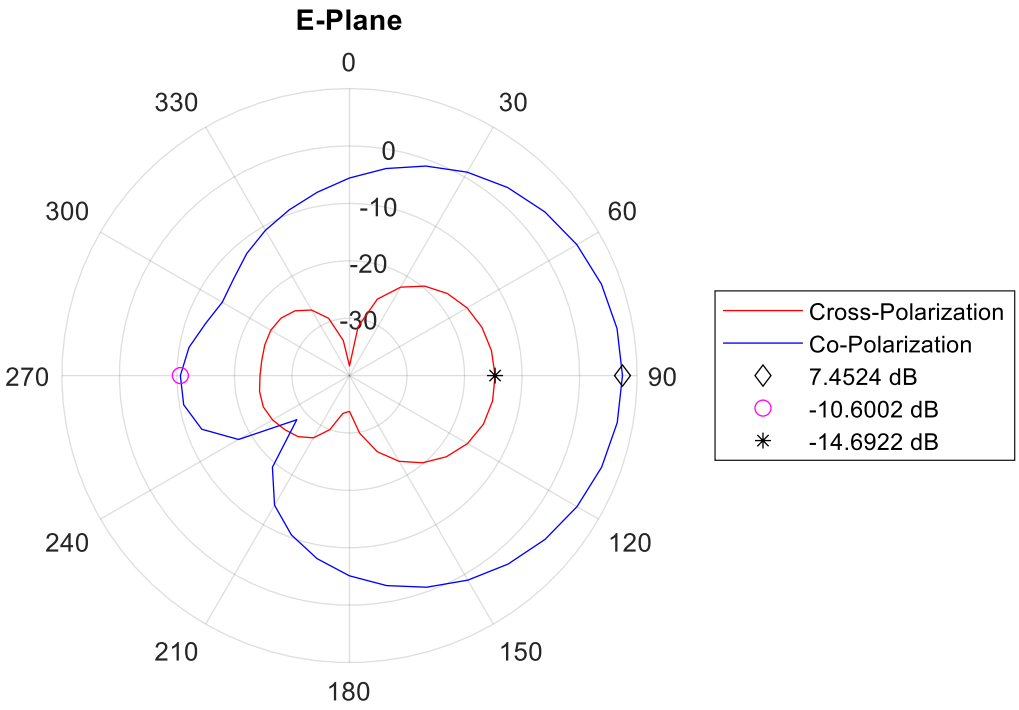

Figure 3.26: Microstrip Filtering Antenna Radiation Pattern E-Plane When Port 1 is Excited

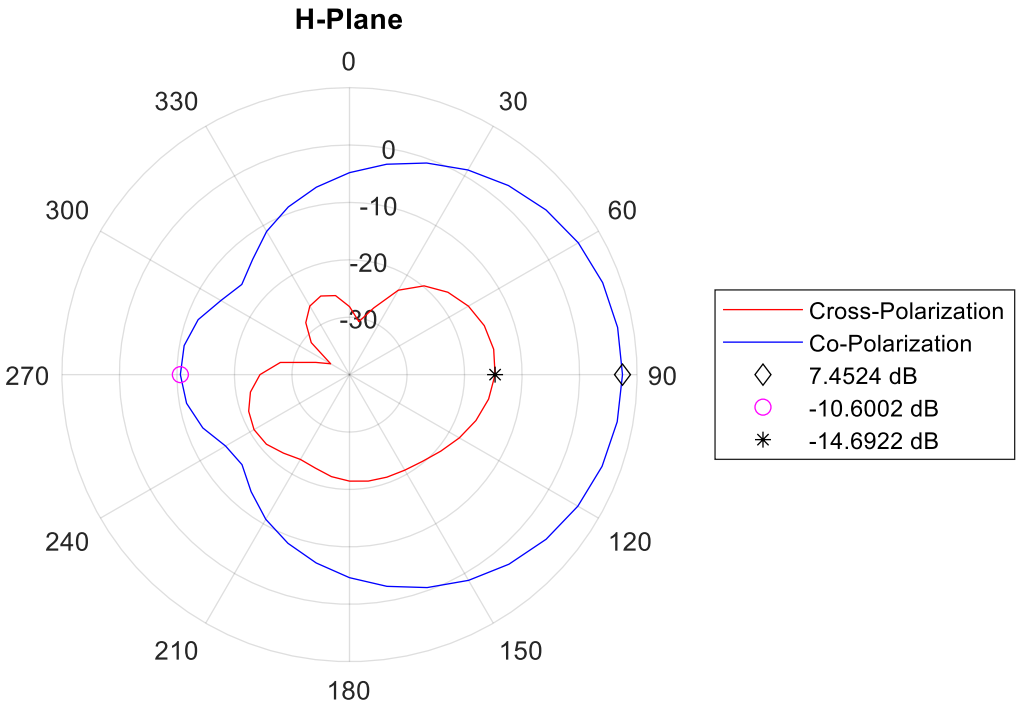

Figure 3.27: Microstrip Filtering Antenna Radiation Pattern H-Plane When Port 1 is Excited

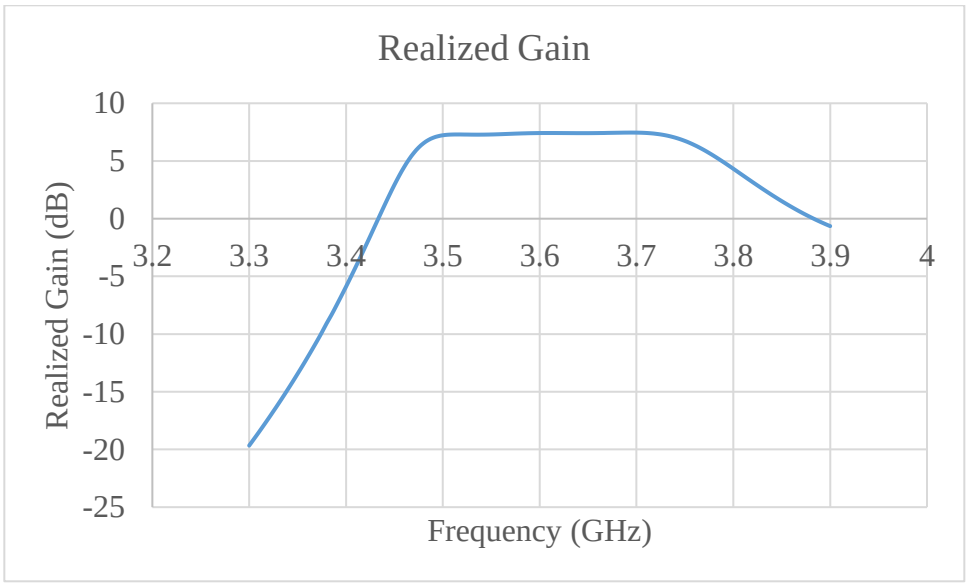

Figure 3.28: Microstrip Filtering Antenna Realized Gain When Port 1 is Excited

Filtering Antenna Characteristics When Port 2 is Excited:

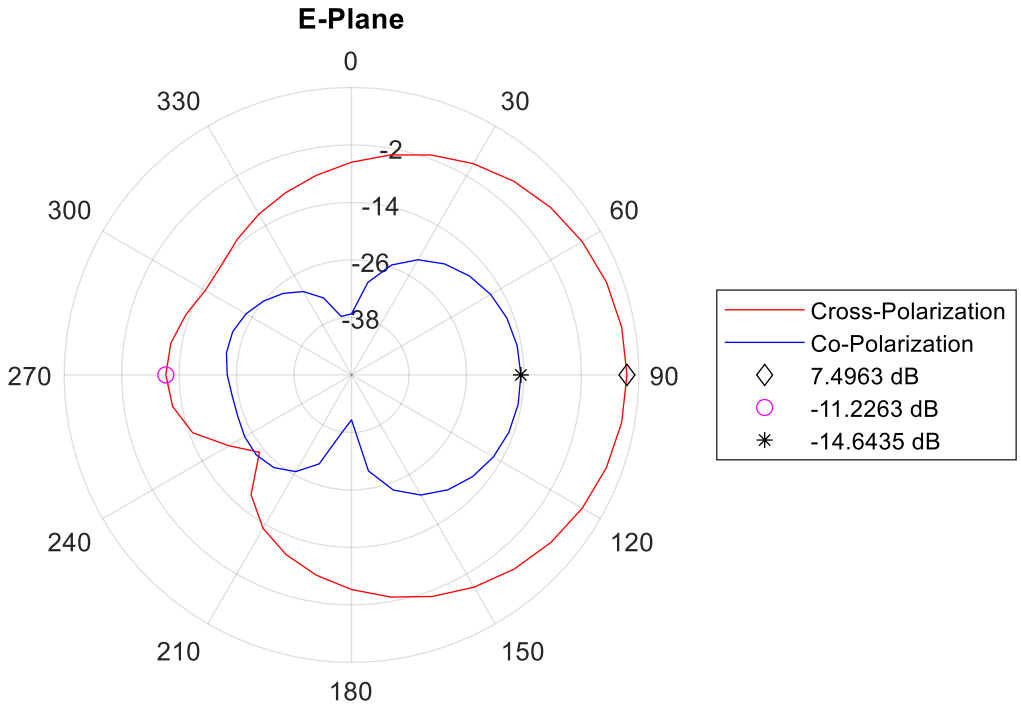

Figure 3.29: Microstrip Filtering Antenna Radiation Pattern E-Plane When Port 2 is Excited

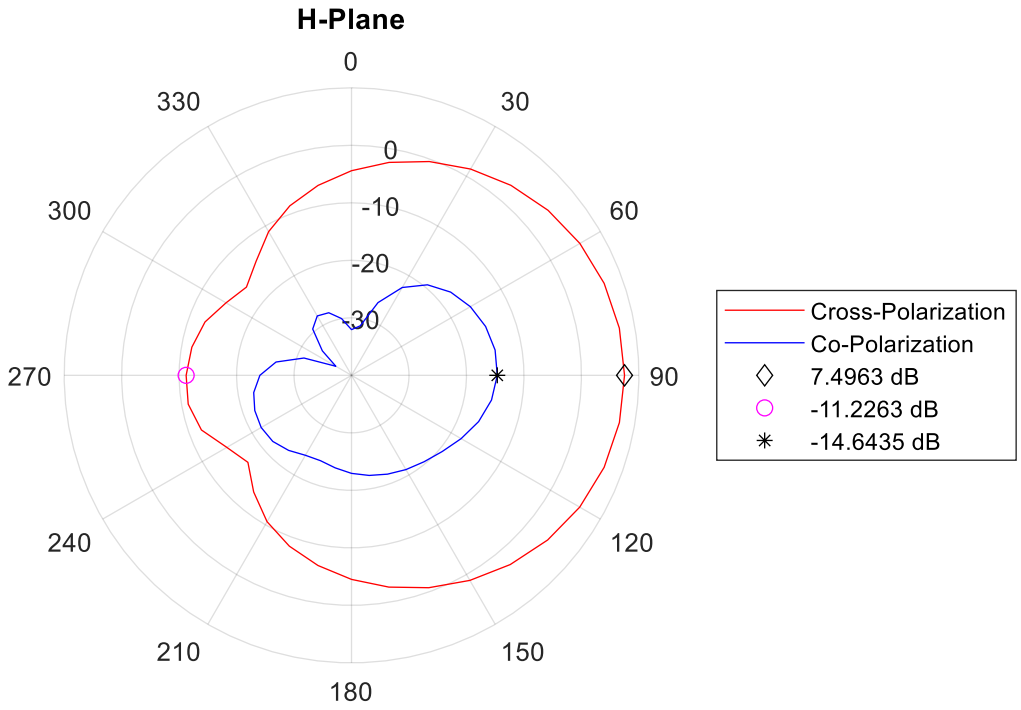

Figure 3.30: Microstrip Filtering Antenna Radiation Pattern H-Plane When Port 2 is Excited

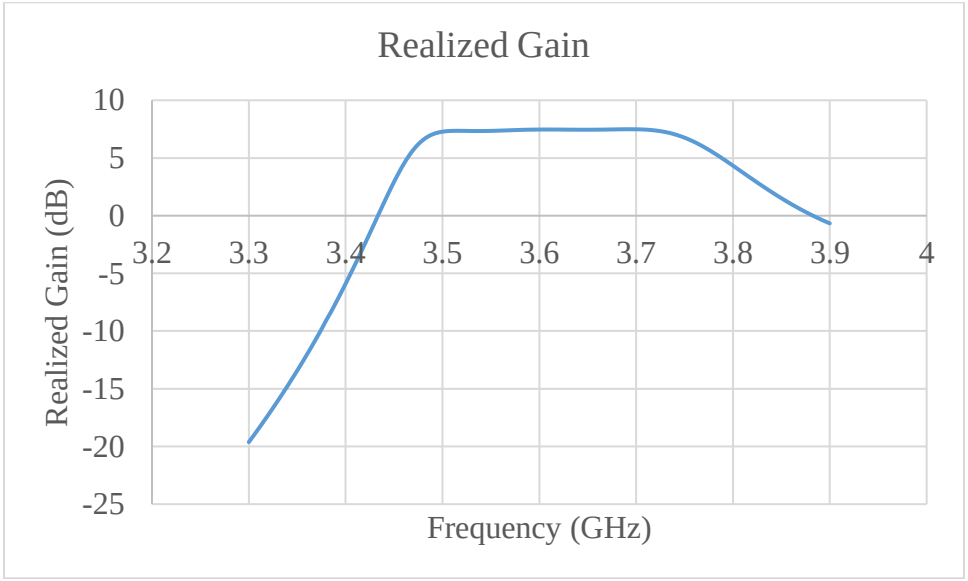

Figure 3.31: Microstrip Filtering Antenna Realized Gain When Port 2 is Excited

Based on the results shown on Figures 3.24 and 3.25, the $|S_{11}|$ of the filtering antenna is better than -17.5 dB from 3.5 GHz to 3.7 GHz and port isolation is greater than 21 dB over the same frequency range. Three resonances are shown in the S_{11} response of the structure; this occurs due to the microstrip antenna bandwidth being similar to the filter bandwidth. In this case, the antenna acts as a resonator with a radiation resistance. The results displayed in Figures 3.26 – 3.31 indicate that the gain of the structure for both polarizations is 7.5 dB, and the realized gain is 7.4 dB, from 3.5 GHz to 3.7 GHz.

3.6 Summary

This chapter discusses the theory and design of the dual-mode waveguide filter and dual polarized microstrip antenna. First, a detailed explanation of the dual-mode waveguide filter and dual polarized microstrip antenna, respectively, is presented. The filter antenna integration procedure is then described. Lastly, the results of the microstrip filtering antenna are given.

Chapter 4

Dielectric Resonator Filtering Antenna

In this chapter, the theory and design of the dual polarized dielectric resonator (DR) filtering antenna is pursued. The same three-pole bandpass waveguide filter with dual-mode presented in chapter 3 is used. This chapter starts with a quantitative explanation of the design of dielectric resonator antenna (DRA). A parametric analysis of various dimensions of the DRA is carried out. Results of the DR filtering antenna structure are presented and discussed. In the end of this chapter, a comparison between the microstrip and DR filtering antennas is shown.

4.1 Design of Dielectric Resonator Antenna (DRA)

The DRA is also an excellent candidate for 5G applications due to its low profile, ease of fabrication and light weight. A square shape is selected and a waveguide with square cross-section is used to excite the antenna. The antenna is designed to operate at 3.6 GHz; the same frequency as the filter centre frequency. The DRA dielectric constant (ε_r) = 20.

To determine the dimensions of the DRA, the following equations are used [78]:

$$k_x = \frac{\pi}{DRA\_a} \tag{4.1}$$

$$k_y = \frac{\pi}{DRA\_b} \tag{4.2}$$

$$k_z \tan\left(\frac{k_z DRA\_d}{2}\right) = \sqrt{(\varepsilon_r - 1){k_o}^2 - {k_z}^2} \tag{4.3}$$

$$k_x{}^2 + k_y{}^2 + k_z{}^2 = \varepsilon_r k_o{}^2 \qquad (4.4)$$

where *DRA_a* is the length, *DRA_d* is the width and *DRA_b* is the height of the DRA. Also, k_o represents the free-space wavenumber corresponding to the resonant frequency. The 3D model of the DRA is shown in Figure 4.1.

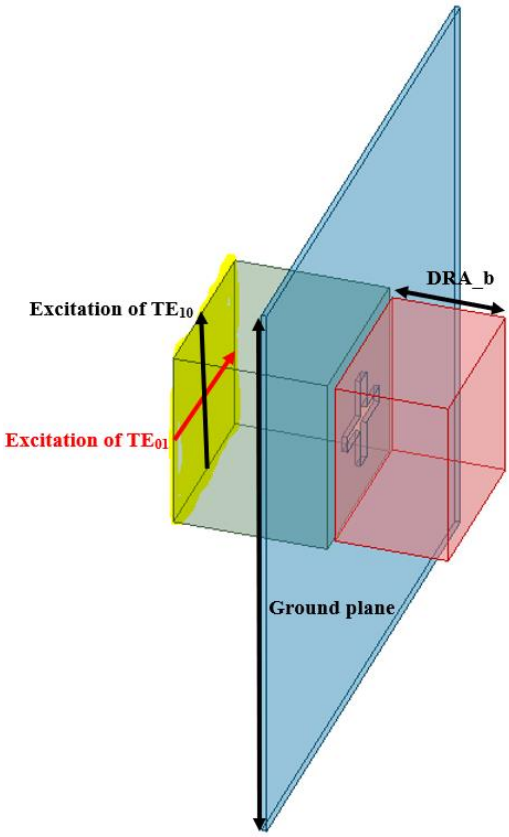

(a) Isometric View

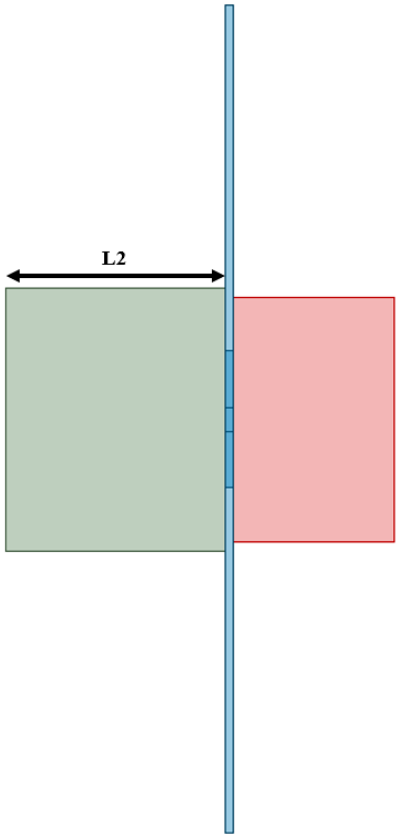

(b) Front View

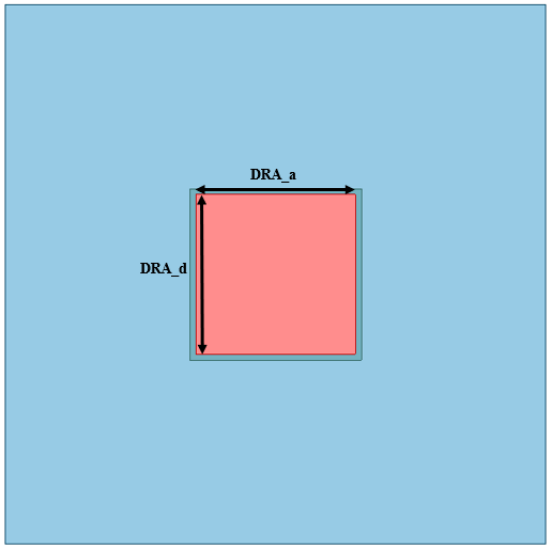

(c) Right Side View

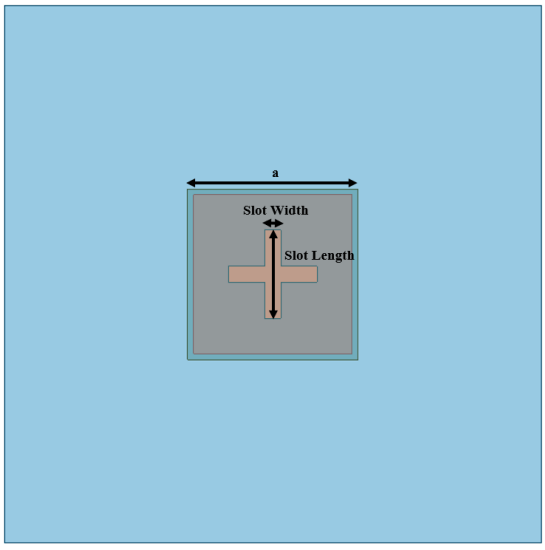

(d) Left Side View

Figure 4.1: DRA Model (a) Isometric View (b) Front Side (c) Right Side View (d) Left Side View

4.2 Parametric Study for DRA and Filter Integration

DRA design parameters such as slot length, slot width, and DRA height affect the coupling between antenna and the filter resonator (K_{23}) as well as the antenna Q_{EXT}. As shown in chapter 3, equations (3.14) – (3.20) are used to calculate K_{23} and Q_{EXT}. The effect of varying DRA heights on K_{23} and Q_{EXT} is shown in Figures 4.2 and 4.3, respectively. Similar to the analysis shown in chapter 3, a parametric analysis of both slot length and slot width is done in three cases. In the first case, a slot width of 1.5 mm is selected and the impact of varying slot lengths on antenna K_{23} and Q_{EXT} is studied. The analysis is shown in Figures 4.4 and 4.5. In the second case, a slot width of 1 mm is selected and again, the impact of varying slot lengths is studied; the results are displayed in Figures 4.6 and 4.7. In the last case, a slot width of 0.5 mm is selected and results from changing slot lengths are shown in Figures 4.8 and 4.9.

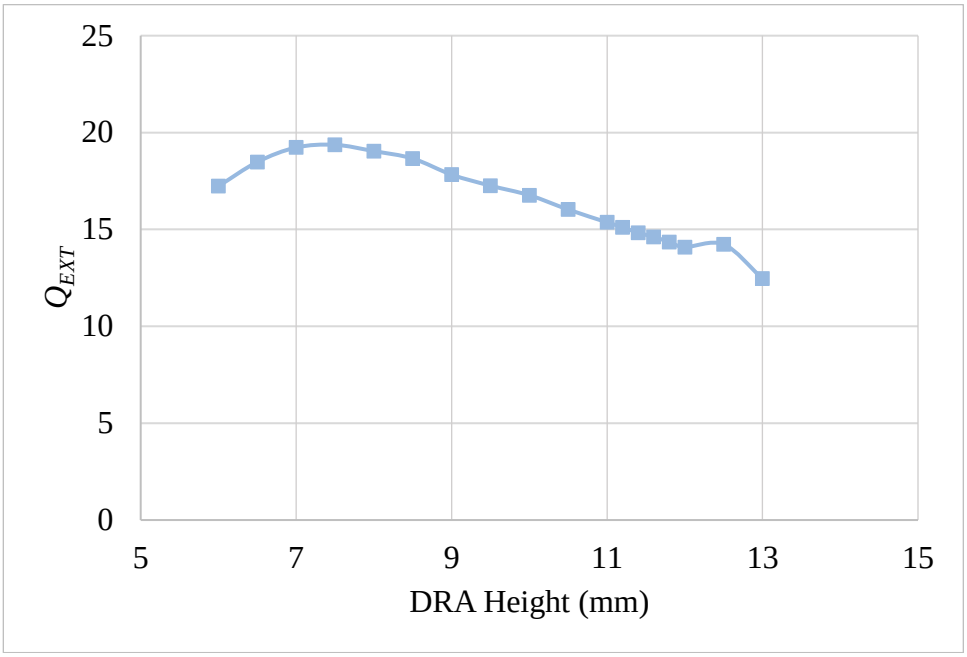

Figure 4.2: The impact of DRA Height variation on Q_{EXT}, where slot length = 7.25 mm and slot width = 1.3 mm

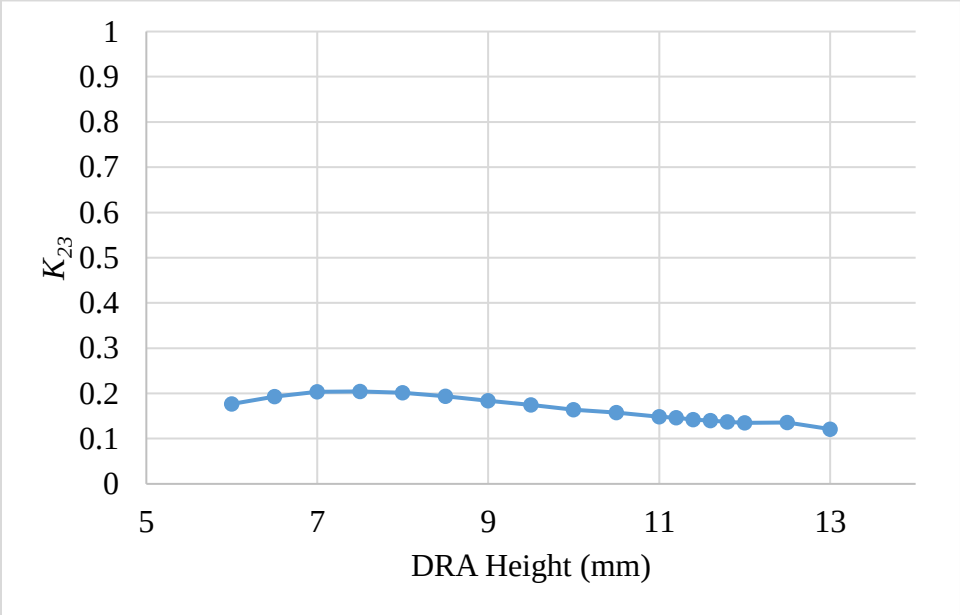

Figure 4.3: The impact of DRA Height variation on K_{23}, where slot length = 7.25 mm and slot width = 1.3 mm

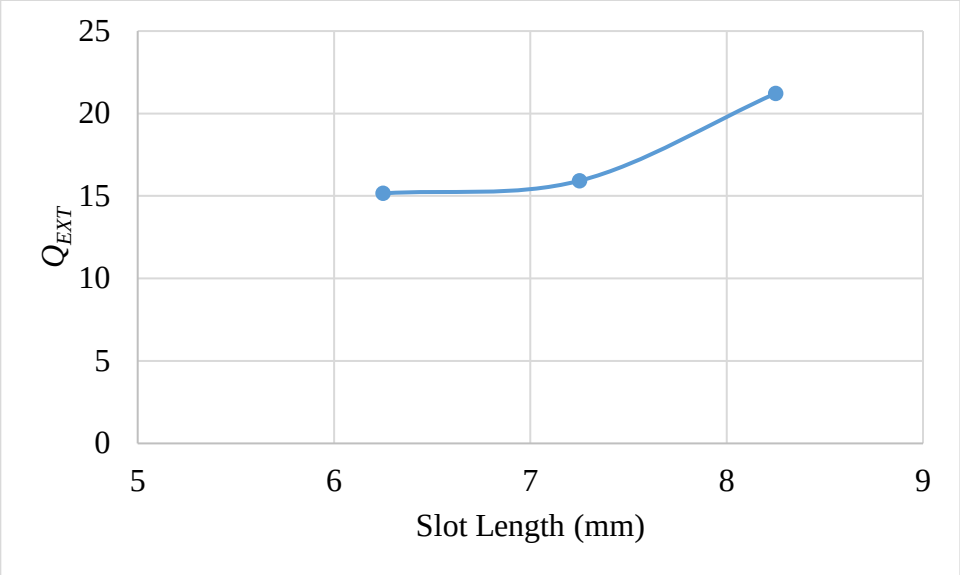

Figure 4.4: The impact of slot length variation on Q_{EXT}, where slot width = 1.5 mm and DRA height = 11 mm

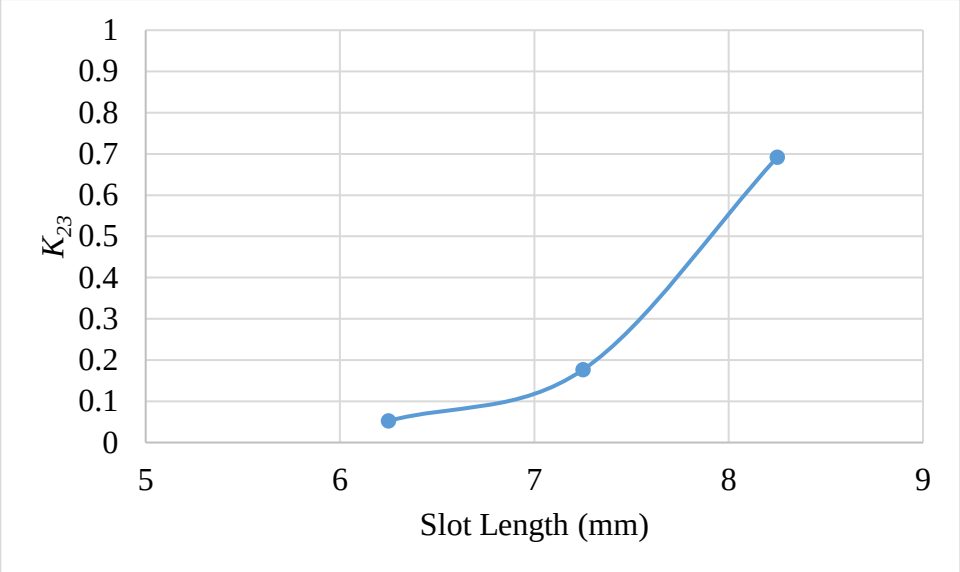

Figure 4.5: The impact of slot length variation on K_{23}, where slot width = 1.5 mm and DRA height = 11 mm

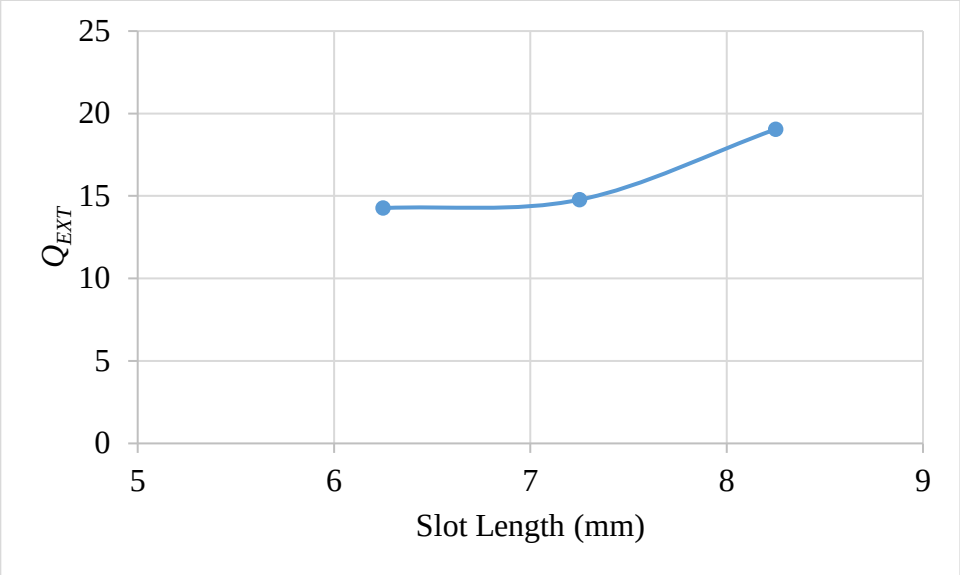

Figure 4.6: The impact of slot length variation on Q_{EXT}, where slot width = 1 mm and DRA height = 11 mm

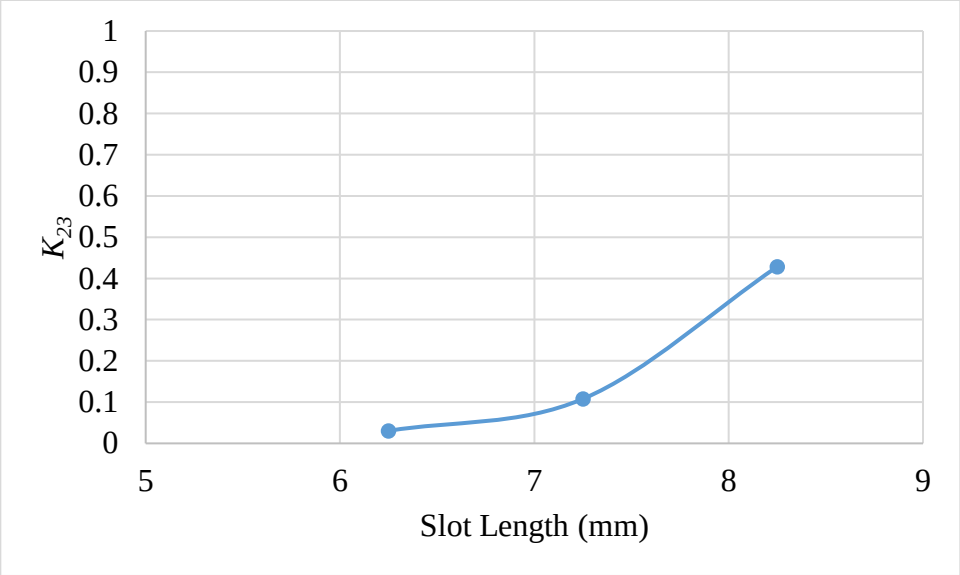

Figure 4.7: The impact of slot length variation on K_{23}, where slot width = 1 mm and DRA height = 11 mm

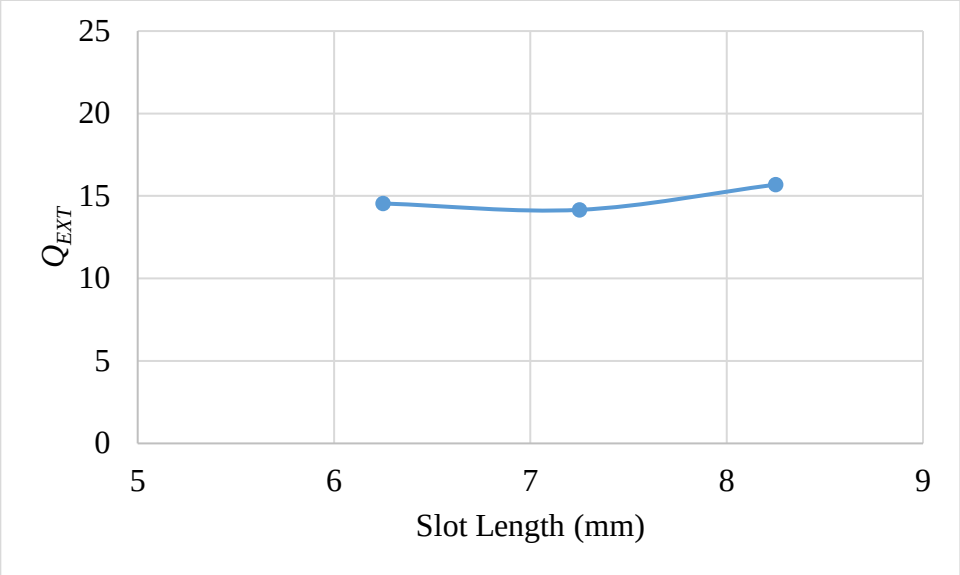

Figure 4.8: The impact of slot length variation on Q_{EXT}, where slot width = 0.5 mm and DRA height = 11 mm

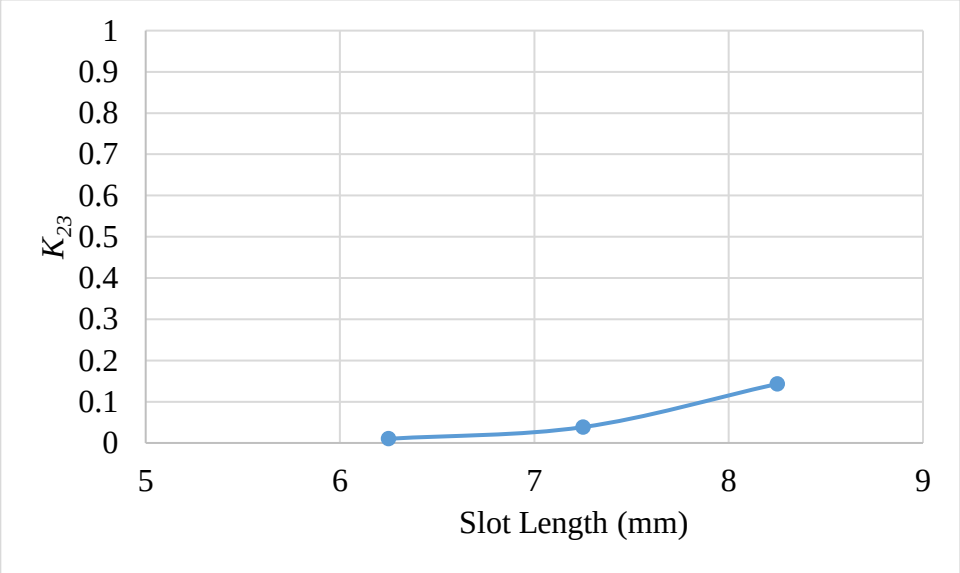

Figure 4.9: The impact of slot length variation on K_{23}, where slot width = 0.5 mm and DRA height = 11 mm

Based on the analysis shown above, it is observed that as the DRA height increases, Q_{EXT} and K_{23} increase until the DRA height is 7.5 mm; when the height is greater than 7.5 mm, Q_{EXT} and k_{23} slowly decrease. In addition, the Q_{EXT} does not have a large range of variation

comparing to microstrip antenna, and it is more difficult for the DRA to be applied to designs with larger bandwidth. This pattern is illustrated in Figures 4.2 and 4.3. Figures 4.4-4.9 indicate that as the slot length increases, the K_{23} also increases. The Q_{EXT}, however, does not change much with varying slot lengths. Another pattern that is observed is that both, Q_{EXT} and K_{23} is higher as slot width increases. Given these observations, the dimensions shown in Table 4.1 are selected for the DRA.

Following the filter antenna integration process in chapter 3, the equivalent circuit model of the last filter resonator (as shown in Figure 3.13) is used to tune the DRA. This method is used to optimize the DRA length, width and height, as well as the slot length and width. The tuned DRA and last filter resonator S_{11} response is displayed in Figure 4.10. Based on the results displayed in Figure 4.10, it can be seen that the bandwidth of the DRA is similar to the bandwidth of the last filter resonator. Therefore, during the filter antenna integration process, the DRA will act as a resonator.

Using equations (3.17)-(3.20) presented in Chapter 3 and the S_{11} response of the DRA, the following values are calculated:

S_{11}^{min} = 0.742

f_0 = 3.6 GHz

f_1 = 3.485 GHz

f_2 = 3.754 GHz

S_{11}^{Φ} = 0.88

Given the values, the Q_{EXT} =15.36 and K_{23} = 0.148, which is similar to the required filter Q_{EXT} = 15.32 and K_{23} = 0.163.

The radiation patterns for both E-plane and H-plane are displayed in Figures 4.11 and 4.12, respectively. The gain of the DRA is 6.8 dB. Due to the symmetric nature of this antenna, the S_{11} response and radiation patterns are similar for both polarizations. For this reason, the results of the antenna for when TE_{101} mode is excited in the waveguide are only shown. Later in this chapter, the complete dual-polarized DR filtering antenna model and results are displayed.

Table 4-1: DRA Dimensions

Parameter	**Value**
a	13.98 mm
L2	11.66 mm
Ground plane	44 mm
DRA_a	12.15 mm
DRA_b	11 mm
DRA_d	12.15 mm
Slot Length	7.25 mm
Slot Width	1.3 mm

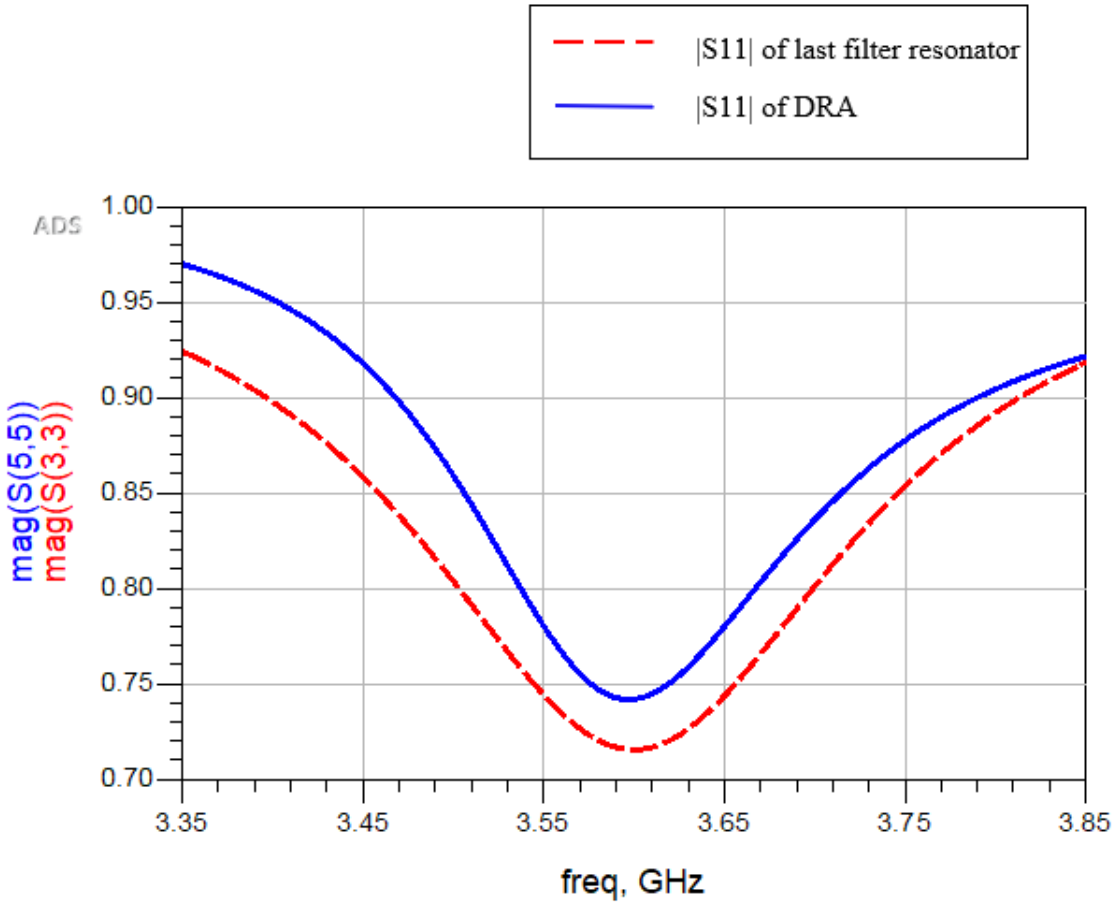

Figure 4.10: $|S_{11}|$ Response of the DRA and Last Filter Resonator

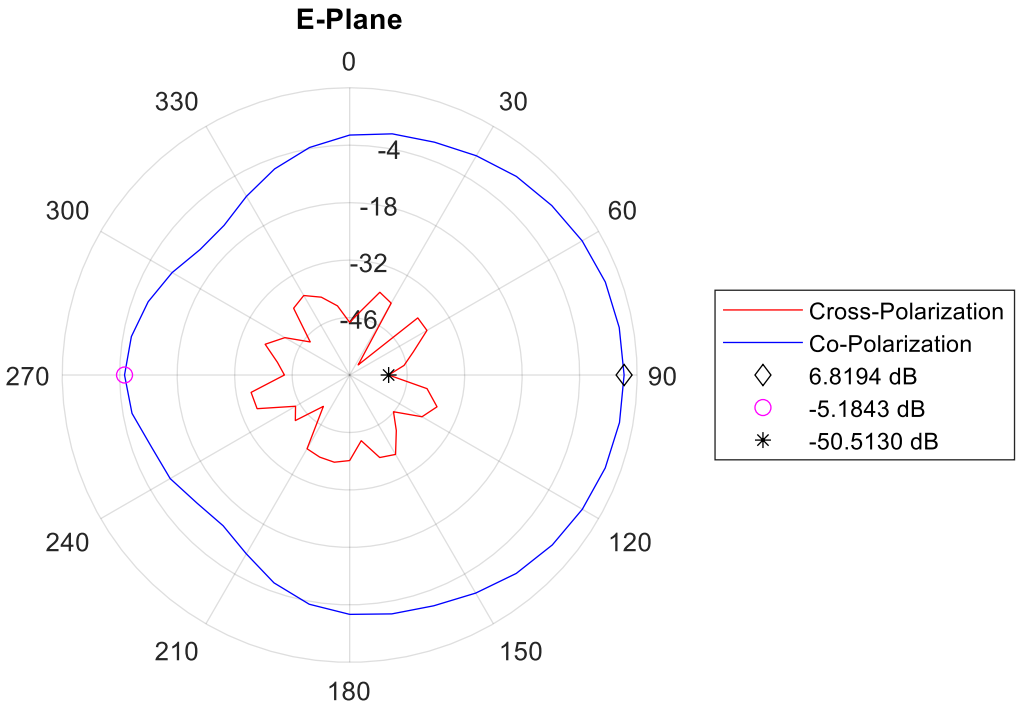

Figure 4.11: DRA Radiation Pattern E-Plane

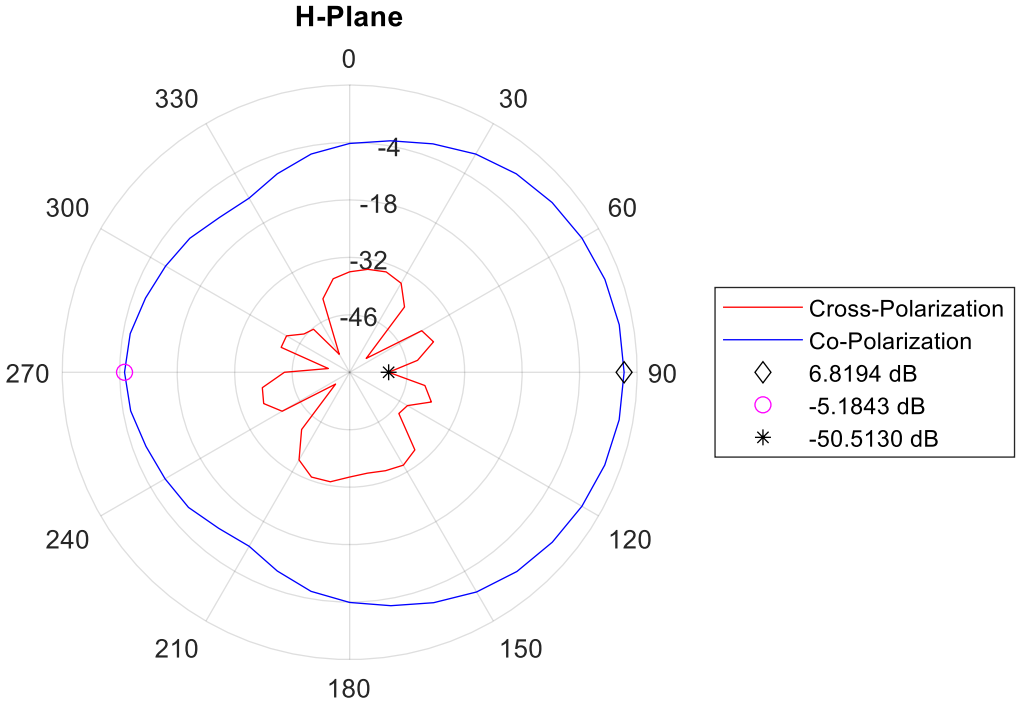

Figure 4.12: DRA Radiation Pattern H-Plane

4.3 Dielectric Resonator Filtering Antenna Simulation Results

Similar to the design process shown in chapter 3, the last step of the DR filtering antenna design process involves the replacement of the last filter resonator with the DRA. Again, the cavity length L2 is fine tuned in this step. The DR slot length and width is also fine-tuned. The dual-polarized dielectric resonator filtering antenna model is shown in Figure 4.13. All of the dimensions of this structure are listed in Table 4.2. Figures 4.14 – 4.23 display results and various characteristics of this structure.

Based on the results shown in Figures 4.14 and 4.15, the $|S_{11}|$ of the filtering antenna is better than -14.11 dB and port isolation is greater than 20 dB from 3.5 GHz to 3.7 GHz. Note that three resonances are shown in the S_{11} response of the structure; this occurs due to the DRA bandwidth being similar to the filter bandwidth. The results given in Figures 4.16 – 4.22 indicate that the gain of the structure, for both polarizations, is 6.7 dB and the cross-polarization is -14 dB.

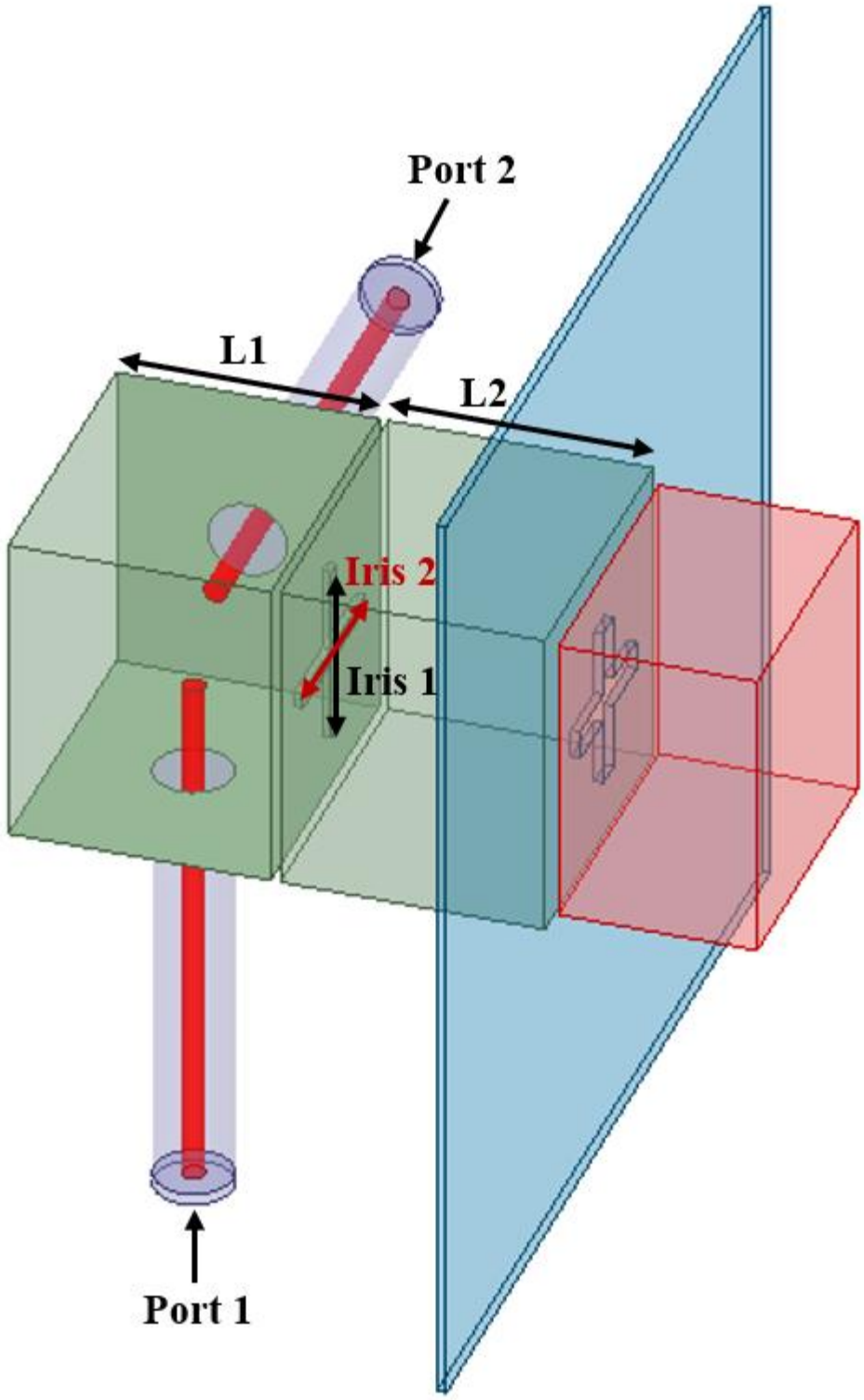

Figure 4.13: Dielectric Resonator Filtering Antenna Model

Table 4-2: DR Filtering Antenna Dimensions

Parameter	**Value**
a	13.98 mm
L1	11.31 mm
L2	11.41 mm
Iris 1	8.02 mm
Iris 2	8.02 mm
Iris_W	0.635 mm
Iris_D	0.4064 mm
DRA_a	12.15 mm
DRA_b	11 mm
DRA_d	12.153 mm
Slot Length	7.46 mm
Slot Width	1.39 mm

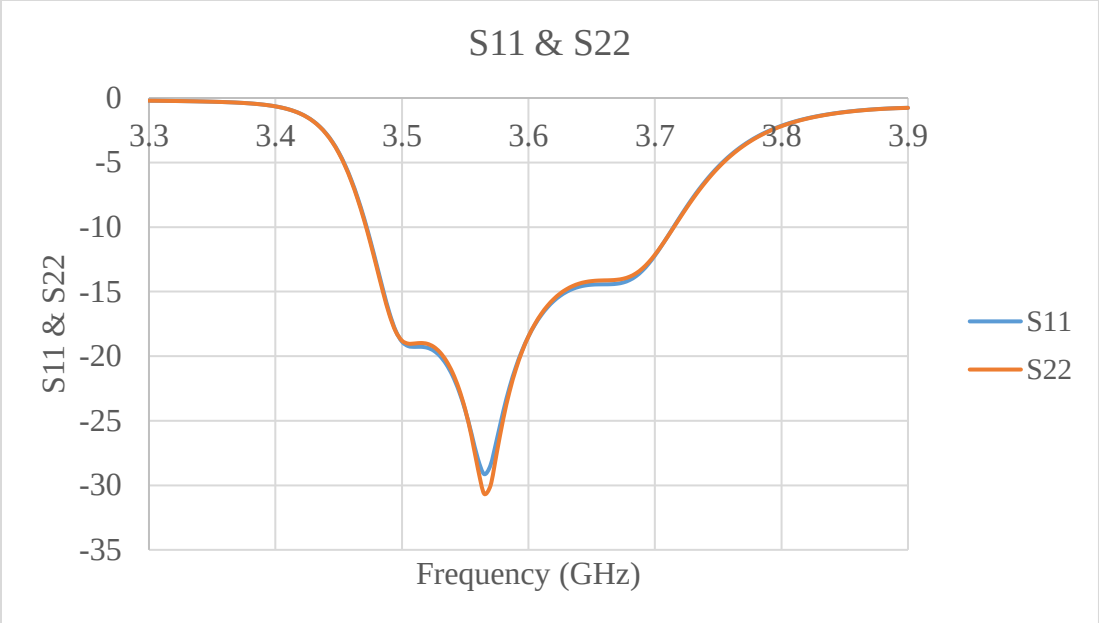

Figure 4.14: DR Filtering Antenna S_{11} and S_{22}

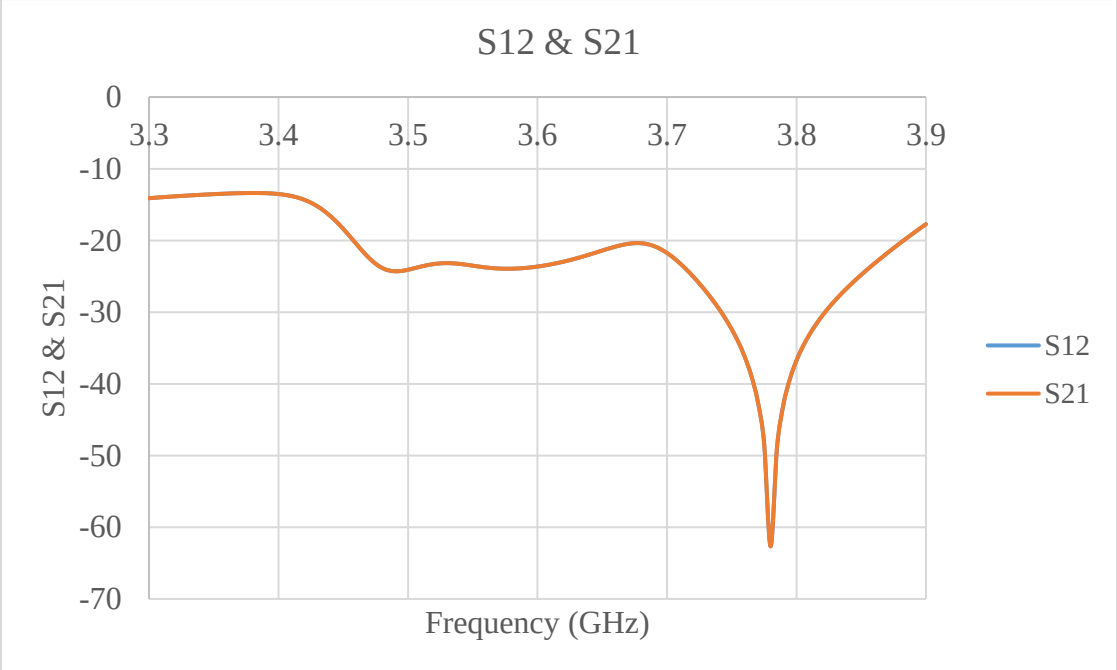

Figure 4.15: DR Filtering Antenna S_{12} and S_{21} Response

Filtering Antenna Characteristics When Port 1 is Excited:

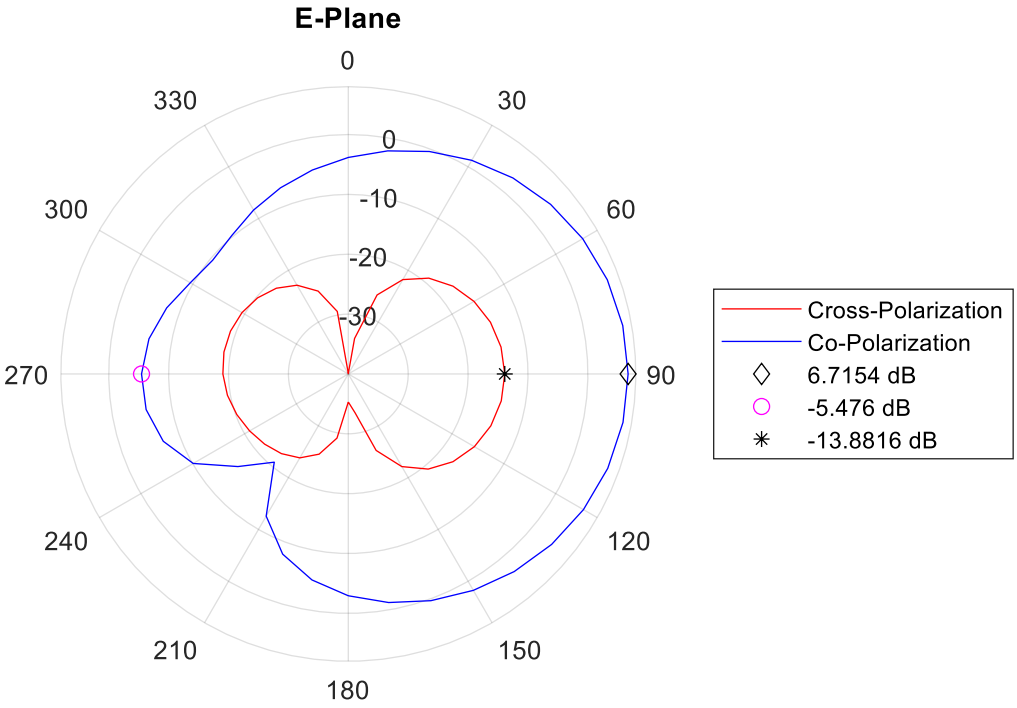

Figure 4.16: DR Filtering Antenna Radiation Pattern E-Plane When Port 1 is Excited

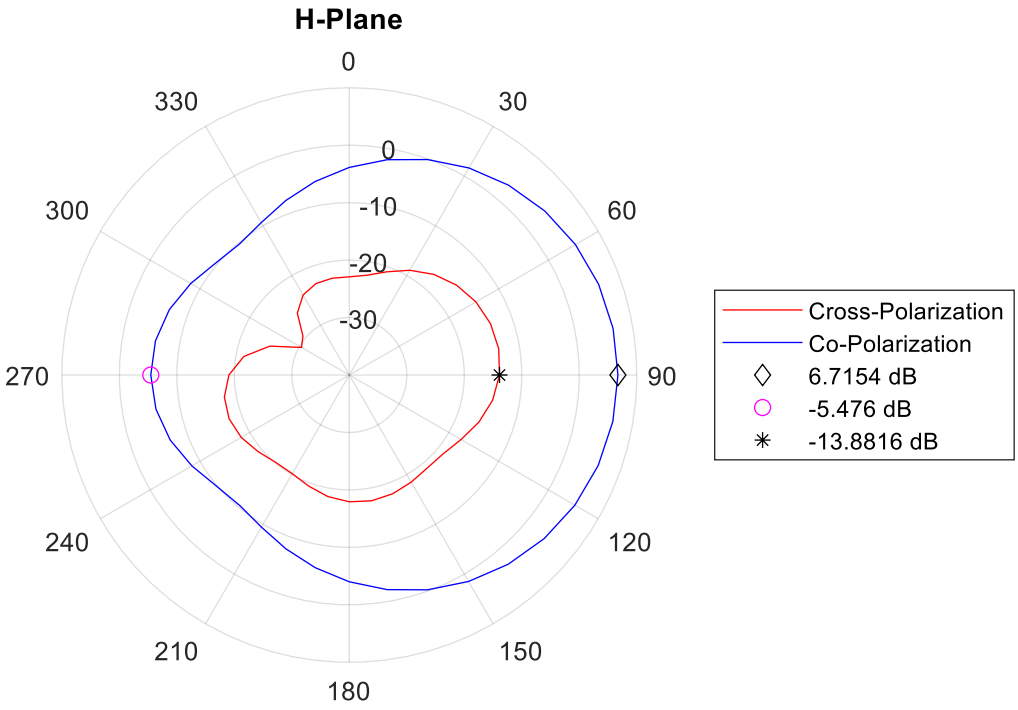

Figure 4.17: DR Filtering Antenna Radiation Pattern H-Plane When Port 1 is Excited

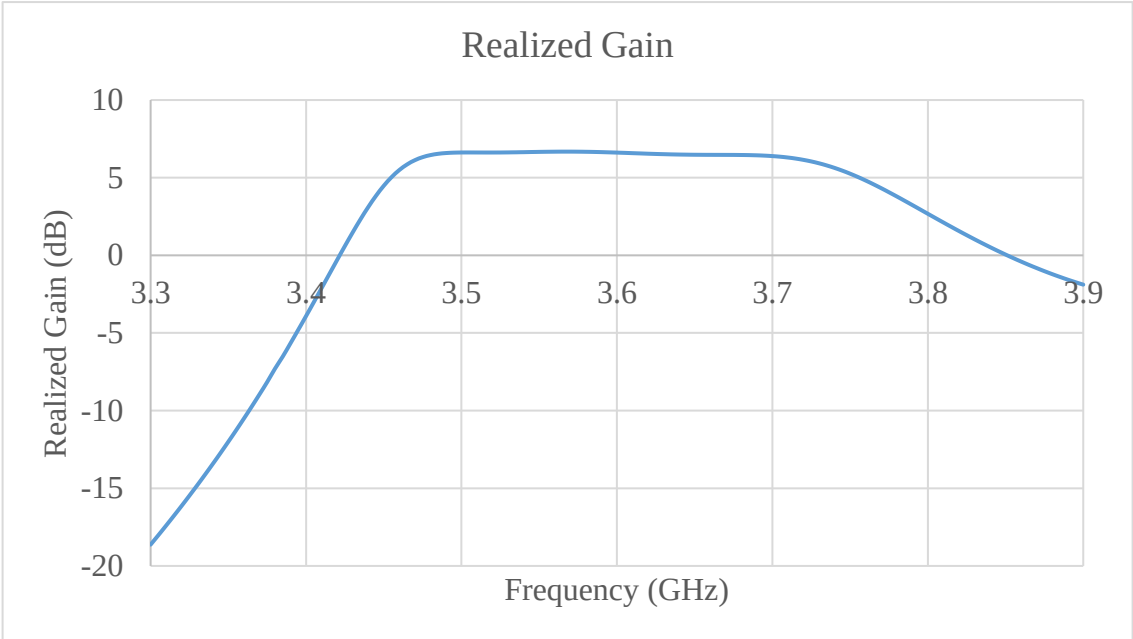

Figure 4.18: DR Filtering Antenna Realized Gain When Port 1 is Excited

Filtering Antenna Characteristics When Port 2 is Excited:

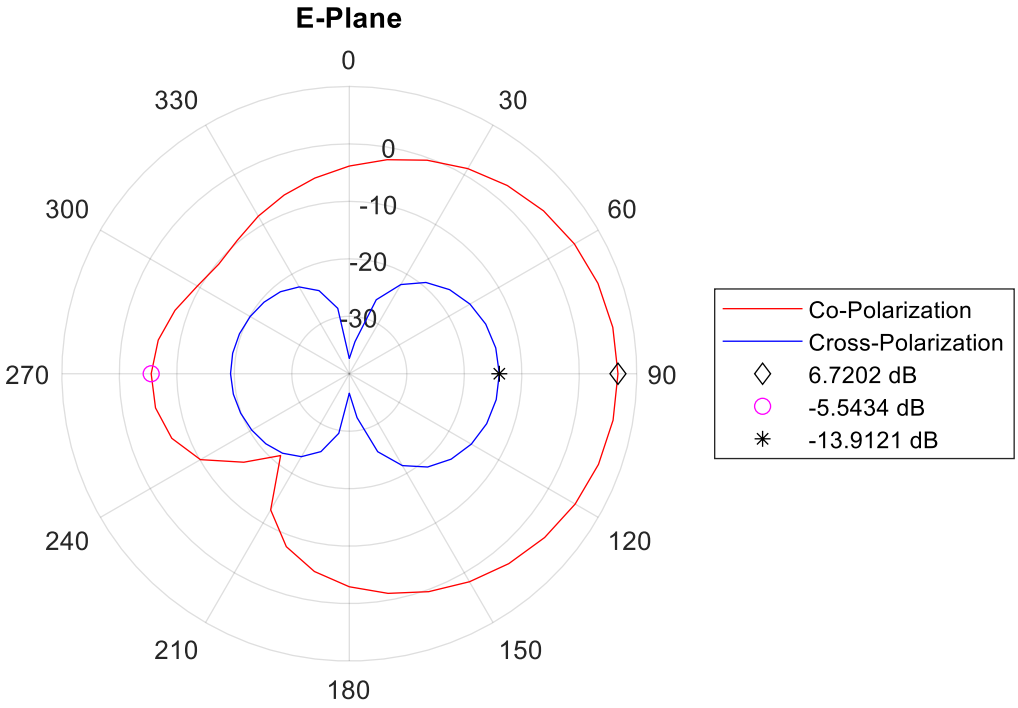

Figure 4.19: DR Filtering Antenna Radiation Pattern E-Plane When Port 2 is Excited

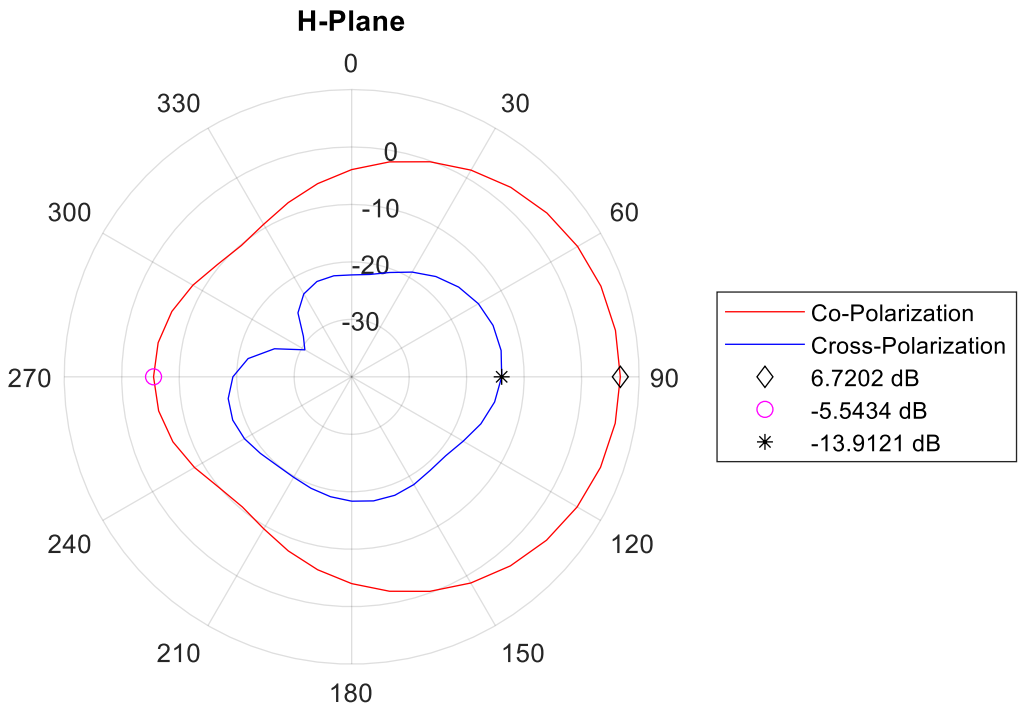

Figure 4.20: DR Filtering Antenna Radiation Pattern H-Plane When Port 2 is Excited

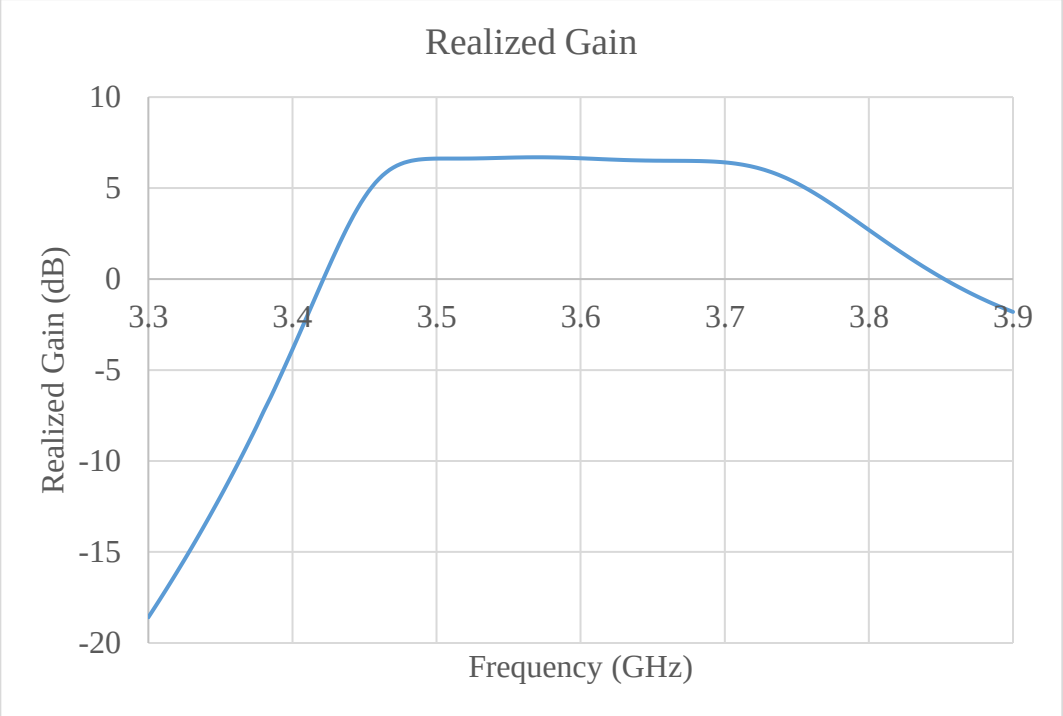

Figure 4.21: DR Filtering Antenna Realized Gain When Port 2 is Excited

4.4 Comparison between Microstrip and Dielectric Resonator Filtering Antennas

In this section, a comparison study is performed between the microstrip and DR filtering antennas. The microstrip filtering antennas presented in chapter 3 (Figure 3.25) and the DR filtering antenna shown in chapter 4 (Figure 4.13) are used for this study. For purpose of this study, a copper material is assigned to the ground plane and the patch of the microstrip antenna. A loss tangent $\tan\delta = 5.625*10^{-5}$ is assigned to the DRA and again, copper material is used for the ground plane of this antenna.

Results and various other characteristics of the filtering antennas (when port 1 is excited) are compared in Figures 4.22-4.26. The results are summarized in Table 4.3. Note that these figures are similar to the ones reported in chapter 3, and previous sections in chapter 4. The difference is that the material losses are included in the figures in this section.

The results indicate that the microstrip filtering antenna has a slightly larger gain than the DR filtering antenna. Both designs have a bandwidth of 200 MHz and a high radiation efficiency of 99%. The DRA has a size of 12.15 mm x 12.15 mm x 11 mm, showing a much smaller footprint than the microstrip antenna with a patch size of 24 mm x 24 mm. However the DRA has larger profile/thickness, and is difficult to be applied for a design with much wider bandwidth.

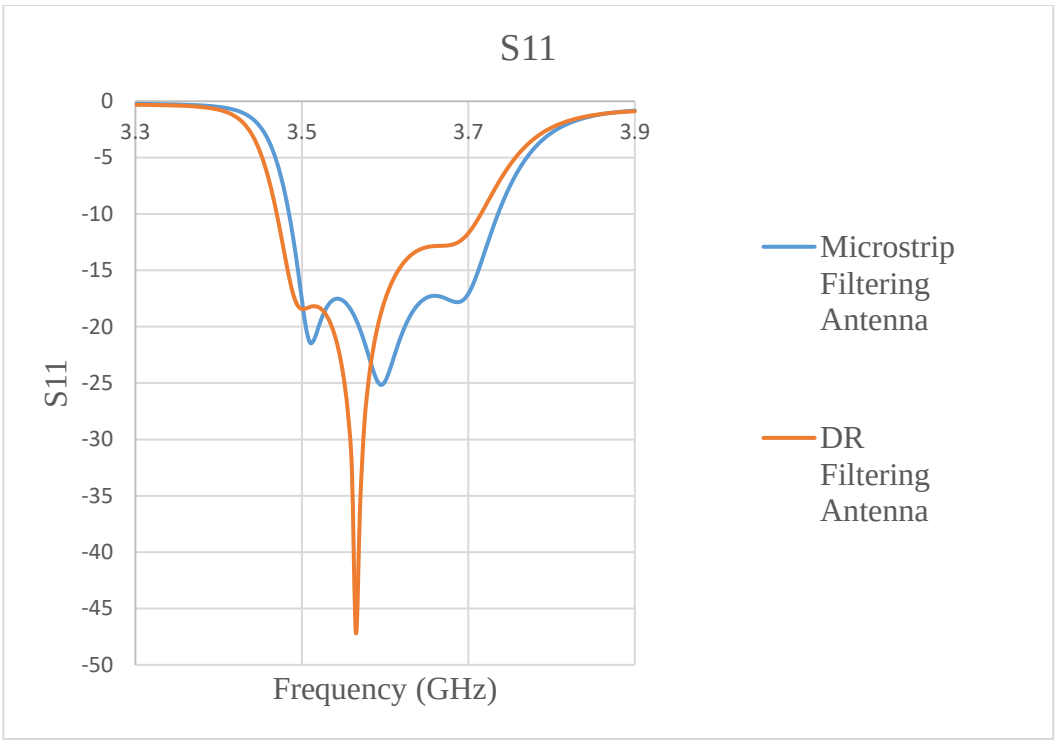

Figure 4.22: S_{11} Response of Microstrip and DR Filtering Antennas When Port 1 is Excited

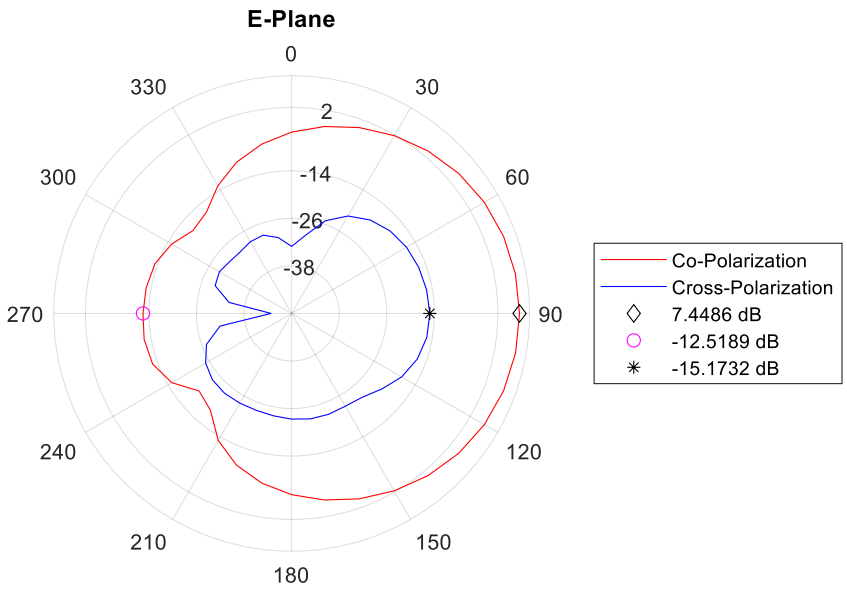

(a)

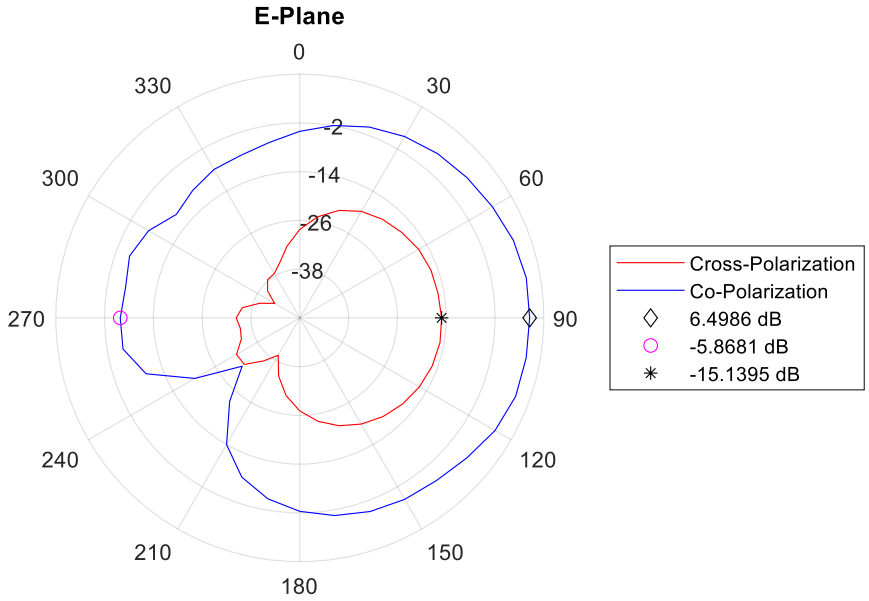

(b)

Figure 4.23: (a) Microstrip and (b) DR Filtering Antenna Radiation Patterns E-Plane When Port 1 is Excited

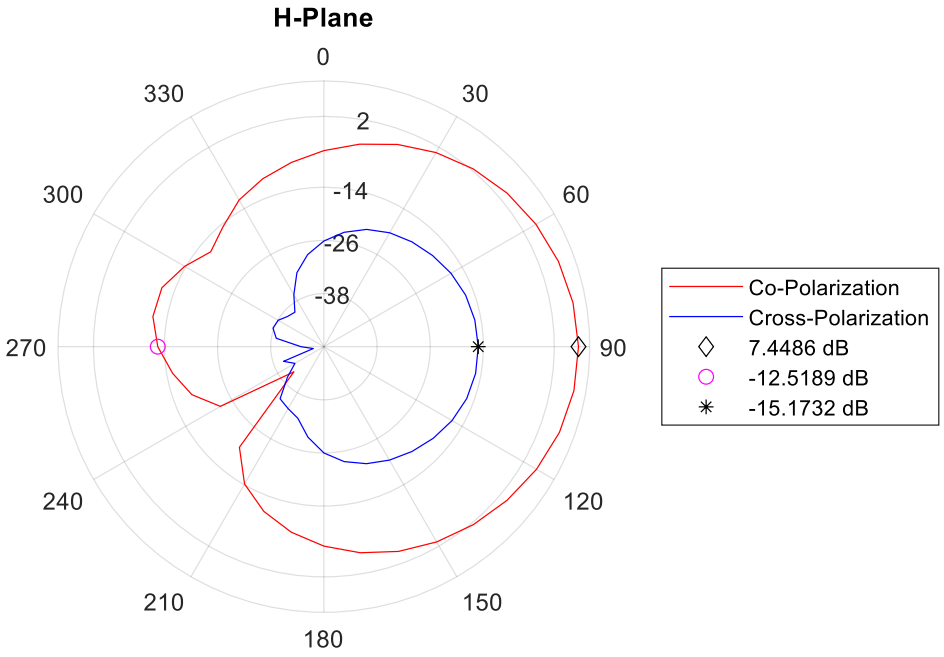

(a)

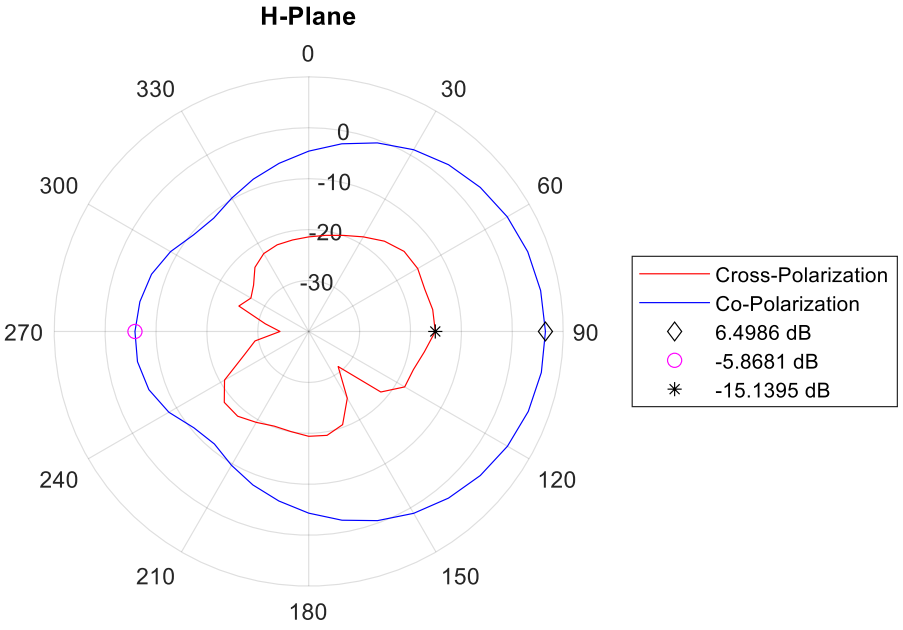

(b)

Figure 4.24: (a) Microstrip and (b) Filtering Antenna Radiation Patterns H-Plane When Port 1 is Excited

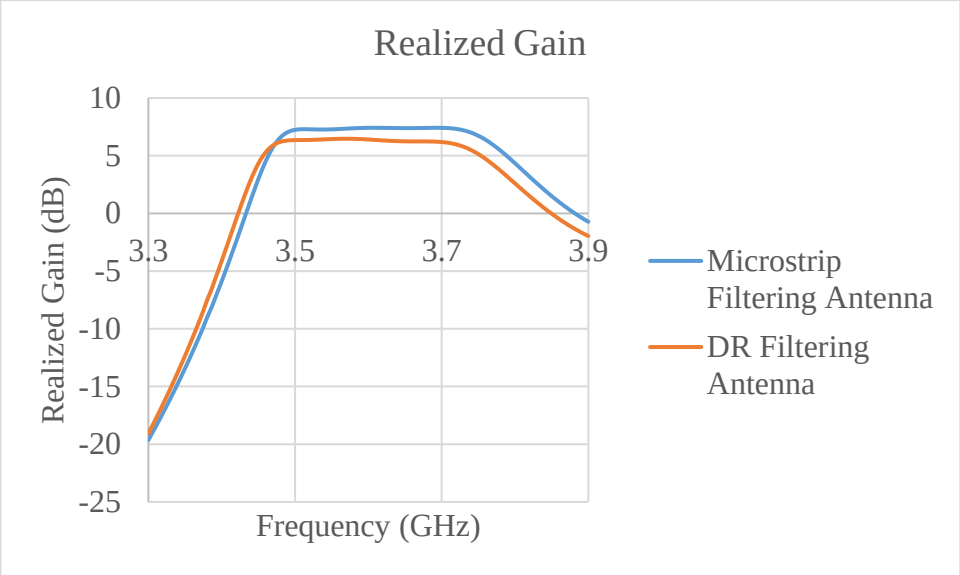

Figure 4.25: Filtering Antenna Realized Gain When Port 1 is Excited

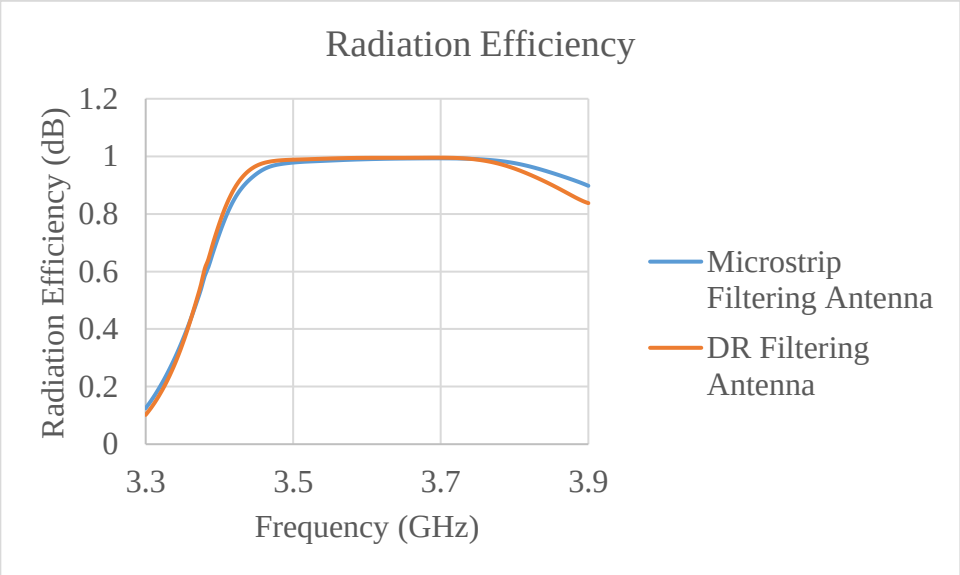

Figure 4.26: Filtering Antenna Radiation Efficiency When Port 1 is Excited

Table 4-3: Comparison between Microstrip and DR Filtering Antennas

Parameter	Microstrip Filtering Antenna	Dielectric Resonator Filtering Antenna
Bandwidth	200 MHz	200 MHz
Gain	7.45 dB	6.50 dB
Realized Gain	7.42 dB	6.41 dB
Radiation Efficiency	99%	99%

4.5 Summary

This chapter discusses the theory and design of the dual polarized DRA. A parametric study of the DRA is presented. Once the ideal dimensions of the DRA are selected, the filter antenna procedure begins. A description of the filter antenna integration procedure is presented. Once the integration process is completed, the results of the DR filtering antenna are shown. Lastly, a comparison between both, the microstrip and DR filtering antennas is given. Conclusions drawn from the comparison are also presented.

Chapter 5

Conclusions and Future Work

Aiming at designs with high compactness and high performance for next generation wireless networks, this thesis focuses on the use of a material with high dielectric constant of approximately 20 and low loss for integrated design of microwave filters and antennas. A material with a high dielectric constant is desirable since it leads to compact designs. At the same time, it causes difficulty and limitations in, for example, the bandwidth of the design.

In typical conventional communication systems, both, antennas and filters are designed separately and then combined via connectors or transmission lines. The usage of interconnecting lines results in the introduction of loss and a degraded filtering antenna system performance. Therefore, to obtain a low-loss filtering antenna, an integrated design approach is used. In this thesis, the method is used for two dual-polarized filtering antenna designs.

In the first dual-polarized filtering antenna design, a waveguide filter and dual microstrip antenna integration in the 3.5 – 3.7 GHz frequency range is presented. Parametric analysis of the microstrip antenna is conducted and the impact of varying antenna dimensions on the external quality factor and coupling coefficient are studied. The filter antenna integration procedure is described. In this design, it is determined that the microstrip antenna has the same bandwidth as the filter. Due to this, the antenna acts as a resonator with a radiation resistance that is integrated to the filter. The dual polarized microstrip

filtering antenna design is design and optimized using a full wave electromagnetic (EM) simulator.

In the second dual-polarized filtering antenna design, a waveguide filter and DRA integration in the same frequency range is presented. Parametric analysis of the DRA is carried out and the impact of varying antenna dimensions is studied. Similar to the microstrip filtering antenna design, the antenna acts as a resonator with a radiation resistance. Full wave EM simulations are results are used to validate the design.

A comparison study between the DR and microstrip filtering antenna was performed. Based on that study it can be concluded that the microstrip antenna has a slightly larger gain. The DR filtering antenna shows smaller footprint, but is difficult to be used for a design with wide bandwidth. Both designs have a high radiation efficiency of 99%.

Future work that can be pursued includes the fabrication and measurement of both microstrip and DR filtering antenna designs. Practical aspects, such as fabrication tolerances, will be investigated. In addition, integration of the dual-mode waveguide filter with a dual polarized DRA or microstrip antenna of a wider bandwidth can be explored. There are different methods that can be implemented to improve antenna bandwidth, including microstrip or DRAs in stacked configurations, placing a varactor diode between the antenna and ground plane while modifying the reverse bias of the varactor to improve microstrip antenna bandwidth, and combining DRAs with microstrip patches or monopoles.

BIBLIOGRAPHY

[1] S. K. Sharma, T. E. Bogale, L. B. Le, S. Chatzinotas, X. Wang and B. Ottersten, "Dynamic Spectrum Sharing in 5G Wireless Networks With Full-Duplex Technology: Recent Advances and Research Challenges," in *IEEE Communications Surveys & Tutorials*, vol. 20, no. 1, pp. 674-707, Firstquarter 2018.

[2] M. Shafi et al., "5G: A Tutorial Overview of Standards, Trials, Challenges, Deployment, and Practice," in *IEEE Journal on Selected Areas in Communications*, vol. 35, no. 6, pp. 1201-1221, June 2017.

[3] M. Simsek, A. Aijaz, M. Dohler, J. Sachs and G. Fettweis, "5G-Enabled Tactile Internet," in *IEEE Journal on Selected Areas in Communications*, vol. 34, no. 3, pp. 460-473, March 2016.

[4] C. A. Balanis, *Antenna Theory Analysis and Design*, 4th ed. New Jersey: John Wiley & Sons, Inc., 2016.

[5] W. Richards, Yuen Lo and D. Harrison, "An improved theory for microstrip antennas and applications," in *IEEE Transactions on Antennas and Propagation,* vol. 29, no. 1, pp. 38-46, January 1981.

[6] D. M. Pozar, "Microstrip antennas," in *Proceedings of the IEEE,* vol. 80, no. 1, pp. 79-91, Jan. 1992.

[7] D. Zheng and K. A. Michalski, "Analysis of arbitrarily shaped coax-fed microstrip antennas with thick substrates," in *Electronics Letters,* vol. 26, no. 12, pp. 794-795, 7 June 1990.

[8] P. Katehi and N. Alexopoulos, "On the modeling of electromagnetically coupled microstrip antennas--The printed strip dipole," in *IEEE Transactions on Antennas and Propagation*, vol. 32, no. 11, pp. 1179-1186, November 1984.

[9] M. P. Purchine and J. T. Aberle, “A Tunable L-Band Circular Microstrip Patch Antenna,” *Microwave Journal*, pp. 80, 84, 87, and 88, October 1994.

[10] R. D. Trivedi and V. Dwivedi, "Stacked Microstrip Patch Antenna: Gain and Bandwidth Improvement, Effect of Patch Rotation," *2012 International Conference on Communication Systems and Network Technologies*, Rajkot, 2012, pp. 45-48.

[11] C. Chen, A. Tulintseff and R. Sorbello, "Broadband two-layer microstrip antenna," *1984 Antennas and Propagation Society International Symposium*, Boston, MA, USA, 1984, pp. 251-254.

[12] S. Long and M. Walton, "A dual-frequency stacked circular-disc antenna," in *IEEE Transactions on Antennas and Propagation*, vol. 27, no. 2, pp. 270-273, March 1979.

[13] W. F. Richards and Y.T. Lo, “Theoretical and Experimental Investigation of a Microstrip Radiator with Multiple Lumped Linear Loads,” *Electromagnetics*, Vol. 3, No. 3-4, pp. 371-385, July-December 1983.

[14] S. Bhardwaj and Y. Rahmat-Samii, "Revisiting the generation of cross-polarization in rectangular patch antennas: A near-field approach," in *IEEE Antennas and Propagation Magazine*, vol. 56, no. 1, pp. 14-38, Feb. 2014.

[15] A. Derneryd, "A theoretical investigation of the rectangular microstrip antenna element," in *IEEE Transactions on Antennas and Propagation*, vol. 26, no. 4, pp. 532-535, July 1978.

[16] A. Derneryd and A. Lind, "Extended analysis of rectangular microstrip resonator antennas," in *IEEE Transactions on Antennas and Propagation*, vol. 27, no. 6, pp. 846-849, November 1979.

[17] D. Chang, "Analytical theory of an unloaded rectangular microstrip patch," in *IEEE Transactions on Antennas and Propagation*, vol. 29, no. 1, pp. 54-62, January 1981.

[18] E. Lier and K. Jakobsen, "Rectangular microstrip patch antennas with infinite and finite ground plane dimensions," in *IEEE Transactions on Antennas and Propagation*, vol. 31, no. 6, pp. 978-984, November 1983.

[19] C. Liu, A. Hessel and J. Shmoys, "Performance of probe-fed microstrip-patch element phased arrays," in *IEEE Transactions on Antennas and Propagation*, vol. 36, no. 11, pp. 1501-1509, Nov. 1988.

[20] D. R. Jackson and N. G. Alexopoulos, "Simple approximate formulas for input resistance, bandwidth, and efficiency of a resonant rectangular patch," in *IEEE Transactions on Antennas and Propagation*, vol. 39, no. 3, pp. 407-410, March 1991.

[21] T. Kim, J. Park and S. Park, "A Theoretical Model for Resonant Frequency and Radiation Pattern on Rectangular Microstrip Patch Antenna on Liquid Crystal Substrate," in *IEEE Transactions on Antennas and Propagation*, vol. 66, no. 9, pp. 4533-4540, Sept. 2018.

[22] Z. Wang, J. Liu and Y. Long, "A Simple Wide-Bandwidth and High-Gain Microstrip Patch Antenna With Both Sides Shorted," in *IEEE Antennas and Wireless Propagation Letters*, vol. 18, no. 6, pp. 1144-1148, June 2019.

[23] N. Liu, L. Zhu, W. Choi and G. Fu, "A Low-Profile Wideband Aperture-Fed Microstrip Antenna With Improved Radiation Patterns," in *IEEE Transactions on Antennas and Propagation*, vol. 67, no. 1, pp. 562-567, Jan. 2019.

[24] A. Petosa and A. Ittipiboon, "Dielectric Resonator Antennas: A Historical Review and the Current State of the Art," in *IEEE Antennas and Propagation Magazine*, vol. 52, no. 5, pp. 91-116, Oct. 2010.

[25] A. Okaya and L. Barash, "The Dielectric Microwave Resonator," in *Proceedings of the IRE*, vol. 50, no. 10, pp. 2081–2092, Oct. 1962.

[26] S. Long, M. McAllister and Liang Shen, "The resonant cylindrical dielectric cavity antenna," in *IEEE Transactions on Antennas and Propagation*, vol. 31, no. 3, pp. 406-412, May 1983.

[27] M. W. McAllister and S. A. Long, "Resonant hemispherical dielectric antenna," in *Electronics Letters*, vol. 20, no. 16, pp. 657-659, 2 August 1984.

[28] M. W. McAllister, S. A. Long and G. L. Conway, "Rectangular dielectric resonator antenna," in *Electronics Letters*, vol. 19, no. 6, pp. 218-219, 17 March 1983.

[29] A. Petosa and S. Thirakoune, "Rectangular Dielectric Resonator Antennas With Enhanced Gain," in *IEEE Transactions on Antennas and Propagation*, vol. 59, no. 4, pp. 1385-1389, April 2011.

[30] A. Petosa, *Dielectric Resonator Antenna Handbook*, Norwood, MA: Artech House, 2007.

[31] W. M. Abdel Wahab, D. Busuioc and S. Safavi-Naeini, "Low Cost Planar Waveguide Technology-Based Dielectric Resonator Antenna (DRA) for Millimeter-

Wave Applications: Analysis, Design, and Fabrication," in *IEEE Transactions on Antennas and Propagation*, vol. 58, no. 8, pp. 2499-2507, Aug. 2010.

[32] K. W. Leung and C. K. Leung, "Wideband dielectric resonator antenna excited by cavity-backed circular aperture with microstrip tuning fork," in *Electronics Letters*, vol. 39, no. 14, pp. 1033-1035, 10 July 2003.

[33] R. Yaduvanshi and H. Parthasarathy, *Rectangular dielectric resonator antennas: theory and design.* New Delhi: Springer, 2015.

[34] A. Petosa, A. Ittipiboon, Y. M. M. Antar, D. Roscoe and M. Cuhaci, "Recent advances in dielectric-resonator antenna technology," in *IEEE Antennas and Propagation Magazine*, vol. 40, no. 3, pp. 35-48, June 1998.

[35] R. A. Kranenburg and S. A. Long, "Microstrip transmission line excitation of dielectric resonator antennas," in *Electronics Letters*, vol. 24, no. 18, pp. 1156-1157, 1 Sept. 1988.

[36] K. W. Leung, K. Y. Chow, K. M. Luk and E. K. N. Yung, "Low-profile circular disk DR antenna of very high permittivity excited by a microstripline," in *Electronics Letters*, vol. 33, no. 12, pp. 1004-1005, 5 June 1997.

[37] Kwok-Wa Leung, Kwai-Man Luk, K. Y. A. Lai and Deyun Lin, "Theory and experiment of an aperture-coupled hemispherical dielectric resonator antenna," in *IEEE Transactions on Antennas and Propagation*, vol. 43, no. 11, pp. 1192-1198, Nov. 1995.

[38] K. W. Leung, "Analysis of aperture-coupled hemispherical dielectric resonator antenna with a perpendicular feed," in *IEEE Transactions on Antennas and Propagation*, vol. 48, no. 6, pp. 1005-1007, June 2000.

[39] G. P. Junker, A. A. Kishk and A. W. Glisson, "Input impedance of an aperture coupled dielectric resonator antenna," *Proceedings of IEEE Antennas and Propagation Society International Symposium and URSI National Radio Science Meeting*, Seattle, WA, USA, 1994, pp. 748-751 vol.2.

[40] A. A. Kishk, A. Ittipiboon, Y. M. M. Antar and M. Cuhaci, "Slot excitation of the dielectric disk radiator," in *IEEE Transactions on Antennas and Propagation*, vol. 43, no. 2, pp. 198-201, Feb. 1995.

[41] K. W. Leung, K. M. Luk, K. Y. A. Lai and D. Lin, "Theory and experiment of a coaxial probe fed hemispherical dielectric resonator antenna," in *IEEE Transactions on Antennas and Propagation*, vol. 41, no. 10, pp. 1390-1398, Oct. 1993.

[42] M. Sujatha, R. R. Reddy and N. K. Darimireddy, "Circularly polarized compact wideband slotted cylindrical dielectric resonator antennas," *2017 IEEE International Conference on Antenna Innovations & Modern Technologies for Ground, Aircraft and Satellite Applications (iAIM)*, Bangalore, 2017, pp. 1-5.

[43] K. W. Leung and K. K. So, "Rectangular waveguide excitation of dielectric resonator antenna," in *IEEE Transactions on Antennas and Propagation*, vol. 51, no. 9, pp. 2477-2481, Sept. 2003.

[44] K. W. Leung and K. K. So, "Theory and Experiment of the Wideband Two-Layer Hemispherical Dielectric Resonator Antenna," in *IEEE Transactions on Antennas and Propagation*, vol. 57, no. 4, pp. 1280-1284, April 2009.

[45] Q. Rao, T. A. Denidni and A. R. Sebak, "Broadband compact stacked T-shaped DRA with equilateral-triangle cross sections," in *IEEE Microwave and Wireless Components Letters*, vol. 16, no. 1, pp. 7-9, Jan. 2006.

[46] W. Huang and A. A. Kishk, "Compact wideband multi-layer cylindrical dielectric resonator antennas," in *IET Microwaves, Antennas & Propagation*, vol. 1, no. 5, pp. 998-1005, October 2007.

[47] A. A. Kishk, "Wide-band truncated tetrahedron dielectric resonator antenna excited by a coaxial probe," in *IEEE Transactions on Antennas and Propagation*, vol. 51, no. 10, pp. 2913-2917, Oct. 2003.

[48] A. A. Kishk, Yan Yin and A. W. Glisson, "Conical dielectric resonator antennas for wide-band applications," in *IEEE Transactions on Antennas and Propagation*, vol. 50, no. 4, pp. 469-474, April 2002.

[49] L. Guo, K. W. Leung and Y. M. Pan, "Compact Unidirectional Ring Dielectric Resonator Antennas With Lateral Radiation," in *IEEE Transactions on Antennas and Propagation*, vol. 63, no. 12, pp. 5334-5342, Dec. 2015.

[50] S. Maity and B. Gupta, "Approximate Theoretical Investigations on Isosceles Triangular Dielectric Resonator Antennas and Experimental Validation," in *IEEE Transactions on Antennas and Propagation*, vol. 66, no. 5, pp. 2640-2643, May 2018.

[51] K. P. Esselle and T. S. Bird, "A hybrid-resonator antenna: experimental results," in *IEEE Transactions on Antennas and Propagation*, vol. 53, no. 2, pp. 870-871, Feb. 2005.

[52] M. Lapierre, Y. M. M. Antar, A. Ittipiboon and A. Petosa, "Ultra wideband monopole/dielectric resonator antenna," in *IEEE Microwave and Wireless Components Letters*, vol. 15, no. 1, pp. 7-9, Jan. 2005.

[53] S. Ghosh and A. Chakrabarty, "Ultrawideband Performance of Dielectric Loaded T-Shaped Monopole Transmit and Receive Antenna/EMI Sensor," in *IEEE Antennas and Wireless Propagation Letters*, vol. 7, pp. 358-361, 2008.

[54] M. N. Jazi and T. A. Denidni, "Design and Implementation of an Ultrawideband Hybrid Skirt Monopole Dielectric Resonator Antenna," in *IEEE Antennas and Wireless Propagation Letters*, vol. 7, pp. 493-496, 2008.

[55] Y. Yusuf, H. Cheng and X. Gong, "A Seamless Integration of 3-D Vertical Filters With Highly Efficient Slot Antennas," in *IEEE Transactions on Antennas and Propagation*, vol. 59, no. 11, pp. 4016-4022.

[56] Bosui Liu, Xun Gong and W. J. Chappell, "Applications of layer-by-layer polymer stereolithography for three-dimensional high-frequency components," in *IEEE Transactions on Microwave Theory and Techniques*, vol. 52, no. 11, pp. 2567-2575, Nov. 2004.

[57] Z. Chen, X. Dai and G. Luo, "A new H-slot coupled microstrip filter-antenna for modern wireless communication systems," *2018 International Workshop on Antenna Technology (iWAT)*, Nanjing, 2018, pp. 1-3.

[58] K. Nadaud, D. L. H. Tong and E. Fourn, "Filtering slot antenna using coupled line resonator," *2014 9th European Microwave Integrated Circuit Conference*, Rome, 2014, pp. 556-559.

[59] Lei Zhu, Rong Fu and Ke-Li Wu, "A novel broadband microstrip-fed wide slot antenna with double rejection zeros," in *IEEE Antennas and Wireless Propagation Letters*, vol. 2, pp. 194-196, 2003.

[60] P. V. Sitaraman, V. K. Velidi, V. S. Kumar and A. De, "An integrated filtering slot-coupled microstrip patch antenna using compact dual-mode resonators for future light weight rover in lunar missions," *2017 IEEE Applied Electromagnetics Conference (AEMC)*, Aurangabad, 2017, pp. 1-2.

[61] E. H. Lim and K. W. Leung, "Compact Three-Port Integrated-Antenna-Filter Modules," in *IEEE Antennas and Wireless Propagation Letters*, vol. 8, pp. 486-489, 2009.

[62] Y. Yusuf and X. Gong, "Compact Low-Loss Integration of High-Q 3-D Filters With Highly Efficient Antennas," in *IEEE Transactions on Microwave Theory and Techniques*, vol. 59, no. 4, pp. 857-865, April 2011.

[63] Y. Quéré, C. Quendo, W. El Hajj and C. Person, "A global synthesis tool and procedure for filter-antenna co-design," *2012 15 International Symposium on Antenna Technology and Applied Electromagnetics*, Toulouse, 2012, pp. 1-4.

[64] Q. Wu, X. Zhang and L. Zhu, "Co-Design of a Wideband Circularly Polarized Filtering Patch Antenna With Three Minima in Axial Ratio Response," in *IEEE Transactions on Antennas and Propagation*, vol. 66, no. 10, pp. 5022-5030, Oct. 2018.

[65] Y. Yusuf, H. Cheng and X. Gong, "Co-designed substrate-integrated waveguide filters with patch antennas," in *IET Microwaves, Antennas & Propagation*, vol. 7, no. 7, pp. 493-501, 15 May 2013.

[66] C. Lin and S. Chung, "A Compact Filtering Microstrip Antenna With Quasi-Elliptic Broadside Antenna Gain Response," in *IEEE Antennas and Wireless Propagation Letters*, vol. 10, pp. 381-384, 2011.

[67] G. Mansour, M. J. Lancaster, P. S. Hall, P. Gardner and E. Nugoolcharoenlap, “Design of Filtering Microstrip Antenna Using Filter Synthesis Approach,” Progress in Electromagnetics Research (PIER), vol. 145, 2014, pp. 59-67.

[68] Y. Yusuf and X. Gong, "A vertical integration of high-Q filters with patch antennas with enhanced bandwidth and high efficiency," *2011 IEEE MTT-S International Microwave Symposium*, Baltimore, MD, 2011, pp. 1-4.

[69] L. Li and G. Liu, "A Differential Microstrip Antenna with Filtering Response," in *IEEE Antennas and Wireless Propagation Letters*, vol. 15, pp. 1983-1986, 2016.

[70] W. Duan, X. Y. Zhang, Y. Pan, J. Xu and Q. Xue, "Dual-Polarized Filtering Antenna With High Selectivity and Low Cross Polarization," in *IEEE Transactions on Antennas and Propagation*, vol. 64, no. 10, pp. 4188-4196, Oct. 2016.

[71] P. F. Hu, Y. M. Pan, K. W. Leung and X. Y. Zhang, "Wide-/Dual-Band Omnidirectional Filtering Dielectric Resonator Antennas," in *IEEE Transactions on Antennas and Propagation*, vol. 66, no. 5, pp. 2622-2627, May 2018.

[72] H. Tang, C. Tong, J. Chen, C. Shao, W. Qin and W. Yang, "Differentially SIW TE20-Mode Fed Substrate Integrated Filtering Dielectric Resonator Antenna for 5G Millimeter Wave Application," *2019 IEEE International Conference on Computational Electromagnetics (ICCEM)*, Shanghai, China, 2019, pp. 1-3.

[73] H. Xu, Y. Wang, L. Roy, W. Abdel-Wahab and J. Liu, "Integration of substrate integrated waveguide filter with dielectric resonator antenna," *2017 IEEE International Symposium on Antennas and Propagation & USNC/URSI National Radio Science Meeting*, San Diego, CA, 2017, pp. 1527-1528.

[74] H. Tang, C. Tong and J. Chen, "Differential Dual-Polarized Filtering Dielectric Resonator Antenna," in *IEEE Transactions on Antennas and Propagation*, vol. 66, no. 8, pp. 4298-4302, Aug. 2018.

[75] D. M. Pozar, *Microwave Engineering*, 4th ed. Hoboken, NJ, USA: Wiley, 2011.

[76] J.S. Hong, *Microstrip Filter for RF/Microwave Applications*, 2nd ed. Hoboken, NJ, USA: Wiley, 2011.

[77] R. J. Cameron, C. M. Kudsia, and R. R. Mansour, *Microwave Filters for Communication Systems: Fundamentals, Design, and Applications.* Hoboken, NJ, USA: Wiley, 2007.

[78] R. Kumar Mongia and A. Ittipiboon, "Theoretical and experimental investigations on rectangular dielectric resonator antennas," in IEEE Transactions on Antennas and Propagation, vol. 45, no. 9, pp. 1348-1356, Sept. 1997.